Merentutkimuslaitos
Havsforskninginstitutet
Finnish Institute of
Marine Research

VARIABILITY OF EXCHANGES IN THE NORTHERN SEAS
VEINS
EC - MAST III PROJECT, 1997 - 2000

HYDROGRAPHIC OBSERVATIONS IN DENMARK STRAIT ON THE VEINS EXPEDITION WITH RV ARANDA IN AUGUST-SEPTEMBER 1997

TECHNICAL REPORT

Bert Rudels, Patrick Eriksson, Hannu Grönvall, Riikka Hietala, Jouko Launiainen and Tero Purokoski

No. 39
1999

MERI

Report Series of the Finnish Institute of Marine Research

MERI - Report Series of the Finnish Institute of Marine Research No. 39, 1999

HYDROGRAPHIC OBSERVATIONS IN DENMARK STRAIT ON THE VEINS EXPEDITION WITH RV ARANDA IN AUGUST-SEPTEMBER 1997

TECHNICAL REPORT

Bert Rudels, Patrick Eriksson, Hannu Grönvall, Riikka Hietala,
Jouko Launiainen and Tero Purokoski

MERI - Report Series of the Finnish Institute of Marine Research No. 39, 1999

Cover photo: Tero Purokoski

Publisher:
Finnish Institute of Marine Research
P.O. Box 33
FIN-00931 Helsinki, Finland
Tel: + 358 9 613941
Fax: + 358 9 61394 494
e-mail: surname@fimr.fi

Julkaisija:
Merentutkimuslaitos
PL 33
00931 Helsinki
Puh: 09-613941
Telekopio: 09-61394 494
e-mail: sukunimi@fimr.fi

Copies of this Report Series may be obtained from the library of the Finnish Institute of Marine Research.

Tämän raporttisarjan numeroita voi tilata Merentutkimuslaitoksen kirjastosta.

ISSN 1238-5328 ISBN 951-53-2082-8

CONTENTS

HYDROGRAPHIC OBSERVATIONS IN DENMARK STRAIT ON THE VEINS EXPEDITION WITH RV ARANDA IN AUGUST-SEPTEMBER 1997 - TECHNICAL REPORT 3

APPENDIX A 25

APPENDIX B

This appendix (301 pages) is available upon request from the Finnish Insitute of Marine Research

HYDROGRAPHIC OBSERVATIONS IN DENMARK STRAIT ON THE VEINS EXPEDITION WITH RV ARANDA IN AUGUST-SEPTEMBER 1997

TECHNICAL REPORT

Bert Rudels, Patrick Eriksson, Hannu Grönvall, Riikka Hietala,
Jouko Launiainen & Tero Purokoski

Finnish Institute of Marine Research
PL 33, 00931 Helsinki, FINLAND

ABSTRACT

Denmark Strait is the most important exit for the water masses formed in the Arctic Mediterranean Sea, and supplies a substantial fraction of the North Atlantic Deep Water. Observations obtained on the cruise of the RV Aranda in Denmark Strait in August-September 1997 as part of the European Community programme VEINS indicate that the densest waters crossing the 610m deep sill are mainly drawn from the intermediate waters of the East Greenland Current. The overflow plume is stratified and capped by a less saline layer as it sinks down to 2000m. The retainment of the low salinity lid during the descent implies that the entrainment of ambient water is small and that the downstream evolution of the plume characteristics is due to mixing, within the plume, between the initial overflow waters. The low-salinity, but dense, water of the East Greenland Current flowing southward over the shelf further to the west may cross the shelf break south of the sill and sink down the slope, adding a less dense fraction to the Deep Northern Boundary Current.

1. INTRODUCTION

The thermohaline part of the global oceanic circulation is driven by the combined actions of the weak upwelling and heating of abyssal water occurring over most of the world's oceans, and the renewal of the abyssal water from a few, localised areas of cooling, dense water formation and deep convection. The most conspicuous of these areas are: the Weddell Sea, and the shelves around the Antarctic continent; the Mediterranean Sea; the Labrador Sea; and the Arctic Mediterranean Sea. Amongst these sources the Arctic Mediterranean may well be the most important one. Together with the Labrador Sea Water (LSW), overflow waters from the Arctic Mediterranean form the North Atlantic Deep Water (NADW) which ventilates the deep layers in all the oceans (Worthington, 1976).

The dense water formation in the Arctic Mediterranean occurs in the Nordic Seas (the Greenland, Iceland and Norwegian Seas) and on the shelves of the Arctic Ocean. However, it has been difficult to obtain estimates of the production rates of these dense waters, not to mention assessing the variability of these rates. The VEINS project (Variability of Exchanges in the Nordic Seas) of the EC Mast III programme has been specifically launched to provide a rationale for how the variability of the production of dense water could be monitored. The initial approach is to study the simultaneous exchanges through all the passages between the Nordic Seas and the Arctic Ocean, and between the Nordic Seas and the North Atlantic, to establish key points where a future, limited, monitoring programme could be successful. It would then be possible to provide quantitative information of the time dependence of the input rate of one of the important components of the Global Ocean thermohaline circulation.

As a contribution within the frame of the VEINS programme, RV Aranda of the Finnish Institute of Marine Research conducted an extensive hydrographic survey in the Denmark Strait area in August-September 1997. The Denmark Strait observations were a part of the cruise 12/1997, which has been reported in "Cruise 12/1997 VEINS-Nordic WOCE, Cruise Report, Finnish Institute of Marine Research". During the expedition, CTD observations as well as water sampling for nutrients, oxygen and for anthropogenic tracers such as CFCs and SF_6 were carried out. In addition ship-mounted ADCP (Acoustic Doppler Current Profiler), XCP (Expendable Current Profiler), and meteorological observations were carried out. This report presents the CTD observations made in Denmark Strait. Further analysis of the measurements and quantitative volume transport estimates will be given in a later study. After a short description of the field work (section 2), the data calibration and data presentation are discussed (section 3). Finally, in section 4, some preliminary results are presented. The work on board the ship was carried out by scientists from several institutions, and Table 1 and Table 2 list the participating institutions and scientists respectively.

Participating institutions

Finnish Institute of Marine Research (FIMR)
Department of Analytical and Marine Chemistry, Göteborg University (GUMC)
Department of Meteorology and Oceanography, Stockholm University (SUMO)
Applied Physics Laboratory, University of Washington (UW)
University of Liverpool (UL)

Table 1. Participants

Leg 2. Reykjavik - Isafjördur 18.-29.8.1997		**Leg 3. Isafjördur-Reykjavik 1.-13.9.1997**	
Hannu Grönvall	FIMR	Jouko Launiainen	FIMR
Riikka Hietala	"	Riikka Hietala	"
Tero Purokoski	"	Juha Kivimäki	"
Bert Rudels	"	Tero Purokoski	"
Henry Söderman	"	Bert Rudels	"
Hannu Vuori	"	Hannu Vuori	"
Peter Lundberg	SUMO	Peter Lundberg	SUMO
Tim Fristedt	"	Tim Fristedt	"
Irene Lake	"	Irene Lake	"
Anna Nikolopoulos	"	Anna Nikolopoulos	"
Toste Tanhua	GUMC	Johan Nilsson	"
Anders Olsson	"	Toste Tanhua	GUMC
Ingrid Kubista	"	Anders Olsson	"
Marie Persson	"	Lars Johansson	"
Malcolm Liddicoat	UL	Malcolm Liddicoat	UL
James Girton	UW		

Table 2. List of stations.

Leg 2: Reykjavik-Isafjördur 18.-29.8.1997						
Index	Station name	Latitude	Longitude	Depth	Date	Time
498	VEINS_K2	N67.1498	W023.3643	397	19970902	1153
499	VEINS_K3	N67.2500	W023.4474	654	19970902	1430
500	VEINS_K4	N67.3495	W023.5315	975	19970902	1813
501	VEINS_K5	N67.4507	W024.0180	1287	19970903	0718
502	VEINS_K6	N67.5506	W024.1016	1481	19970903	1127
503	VEINS_K7	N68.0499	W024.1880	1500	19970903	1459
504	VEINS_K10	N68.1891	W025.2846	300	19970903	1935
505	VEINS_K9	N68.1418	W025.0512	729	19970903	2149
506	VEINS_K8	N68.0962	W024.4199	1279	19970904	0134
507	VEINS_H11	N68.0498	W026.1265	312	19970904	0731
508	VEINS_H10	N67.5903	W025.5602	404	19970904	0925
509	VEINS_H9	N67.5296	W025.3993	641	19970904	1128
510	VEINS_H8	N67.4723	W025.2557	1079	19970904	1329

ERRATA

Meri – Report Series of the Finnish Institute of Marine Research No. 39, 1999, p. 4: Table 2. The correct list of stations for the Leg 2 is as follows:

Leg 2: Reykjavik-Isafjördur 18.-29.8.1997						
Index	Station name	Latitude	Longitude	Depth	Date	Time
426	VE_TEST1	N64.1420	W023.2242	106	19970818	1623
427	VEINS_N1	N64.2801	W026.0005	273	19970818	2322
428	VEINS_N2	N64.2658	W026.1834	284	19970819	0102
429	VEINS_N3	N64.2507	W026.3647	325	19970819	0249
430	VEINS_N4	N64.2363	W026.5477	342	19970819	0432
431	VEINS_N5	N64.2219	W027.1291	644	19970819	0617
432	VEINS_N6	N64.2074	W027.3108	862	19970819	0823
433	VEINS_N7	N64.1927	W027.4923	962	19970819	1051
434	VEINS_N8	N64.1782	W028.0737	1243	19970819	1334
435	VEINS_N9	N64.1638	W028.2547	1341	19970819	1618
436	VEINS_N10	N64.1092	W029.3337	1939	19970819	2114
437	VEINS_N11	N64.0544	W030.4097	2611	19970820	0252
438	VEINS_N12	N64.0000	W031.4838	2725	19970820	0900
439	VEINS_N12	N63.5996	W031.4813	2724	19970820	1326
440	VEINS_A1	N63.5492	W032.4943	2609	19970822	0810
441	VEINS_A2	N64.0312	W033.0461	2412	19970822	1318
442	VEINS_A3	N64.1126	W033.1958	2216	19970822	1726
443	VEINS_A4	N64.1940	W033.3469	1985	19970822	2224
444	VEINS_A5	N64.2747	W033.4943	1697	19970823	0237
445	VEINS_A6	N64.3563	W034.0455	1400	19970823	0636
446	VEINS_A7	N64.4377	W034.1952	1152	19970823	1017
447	VEINS_A8	N64.5187	W034.3478	1000	19970823	1319
448	VEINS_A9	N64.5998	W034.4994	341	19970823	1604
449	VEINS_B1	N64.4999	W032.0018	2164	19970824	0033
450	VEINS_B2	N64.5859	W032.0004	1991	19970824	0459
451	VEINS_B3	N65.0721	W032.0002	1750	19970824	0849
452	VEINS_B4	N65.1580	W031.5998	1441	19970824	1221
453	VEINS_B5	N65.2442	W032.0002	1025	19970824	1538
454	VEINS_B6	N65.3301	W032.0002	450	19970824	1821
455	VEINS_D6	N65.2799	W030.2724	409	19970824	2317
456	VEINS_D5	N65.1943	W030.2272	1022	19970825	0144
457	VEINS_D4	N65.1118	W030.1830	1464	19970825	0501
458	VEINS_D3	N65.0250	W030.1384	1820	19970825	0822
459	VEINS_D2	N64.5405	W030.0957	2056	19970825	1202
460	VEINS_J11	N65.0680	W030.3370	1639	19970825	1645
461	VEINS_J10	N65.1163	W030.1695	1447	19970825	1935
462	VEINS_J9	N65.1603	W030.0247	1306	19970825	2209
463	VEINS_J7	N65.2521	W029.3205	1126	19970826	0155
464	VEINS_J6	N65.2977	W029.1676	1122	19970826	0428
465	VEINS_J5	N65.3433	W029.0202	1082	19970826	0640
466	VEINS_J4	N65.3896	W028.4717	1066	19970826	0840
467	VEINS_J3	N65.4355	W028.3200	935	19970826	1039
468	VEINS_J2	N65.4800	W028.1698	762	19970826	1237
469	VEINS_J1	N65.5260	W028.0188	616	19970826	1440
470	VEINS_E1	N65.5900	W028.3200	455	19970826	1747
471	VEINS_E2	N65.5322	W028.2449	548	19970826	1920
472	VEINS_E3	N65.4768	W028.1736	768	19970826	2105

Leg 2: Reykjavik-Isafjördur 18.-29.8.1997						
Index	Station name	Latitude	Longitude	Depth	Date	Time
473	VEINS_E4	N65.4215	W028.0979	906	19970826	2306
474	VEINS_E5	N65.3671	W028.0195	835	19970827	0120
475	VEINS_E6	N65.3116	W027.5446	816	19970827	0344
476	VEINS_E7	N65.2557	W027.4721	800	19970827	0543
477	VEINS_E8	N65.1994	W027.3994	729	19970827	0746
478	VEINS_L9	N66.1902	W027.4507	381	19970827	1527
479	VEINS_L8	N66.1501	W027.3293	497	19970827	1714
480	VEINS_L7	N66.1298	W027.2703	496	19970827	1840
481	VEINS_L6	N66.1098	W027.2099	496	19970827	1958
482	VEINS_L5	N66.0898	W027.1495	537	19970827	2114
483	VEINS_L4	N66.0699	W027.0894	625	19970827	2242
484	ADCP_ICE	N66.0457	W027.0413	677	19970828	0030
485	VEINS_L2	N66.0296	W026.5512	597	19970828	0237
486	VEINS_L1	N66.0102	W026.4800	452	19970828	0437
487	ADCP_ICE	N66.0459	W027.0415	681	19970828	0646
488	VEINS_S10	N66.4793	W027.2303	370	19970828	1201
489	VEINS_S9	N66.4482	W027.1037	408	19970828	1329
490	VEINS_S8	N66.4175	W026.5753	476	19970828	1457
491	VEINS_S7	N66.3864	W026.4503	540	19970828	1637
492	VEINS_S6	N66.3548	W026.3229	567	19970828	1826
493	VEINS_S5	N66.3236	W026.1970	629	19970828	2005
494	VEINS_S4	N66.2924	W026.0711	677	19970828	2153
495	VEINS_S3	N66.2612	W025.5467	656	19970829	0014
496	VEINS_S2	N66.2298	W025.4199	450	19970829	0259
497	VEINS_S1	N66.2143	W025.3573	331	19970829	0436

Index	Station name	Latitude	Longitude	Depth	Date	Time
511	VEINS_H7	N67.4149	W025.1136	1343	19970904	1600
512	VEINS_H6	N67.3565	W024.5694	1449	19970904	1851
513	VEINS_H5	N67.2999	W024.4265	1354	19970904	2210
514	VEINS_H4	N67.2426	W024.2838	1152	19970905	0208
515	VEINS_H3	N67.1854	W024.1423	877	19970905	0512
516	VEIN nnS_H2	N67.1272	W023.5989	568	19970905	0730
517	VEINS_H1	N67.0698	W023.4574	280	19970905	0929
518	VEINS_K1	N67.0496	W023.2737	241	19970905	1100
519	VEINS_R1	N66.4800	W024.5309	579	19970905	1519
520	VEINS_R2	N66.5319	W025.0846	925	19970905	1714
521	VEINS_R2	N66.5270	W025.0955	929	19970905	1820
522	VEINS_R3	N66.5838	W025.2403	1083	19970905	2048
523	VEINS_R4	N67.0359	W025.3947	945	19970906	0009
524	VEINS_R5	N67.0877	W025.5501	835	19970906	0316
525	VEINS_R6	N67.1399	W026.1078	739	19970906	0657
526	VEINS_R7	N67.1924	W026.2628	591	19970906	0905
527	VEINS_R8	N67.2434	W026.4211	293	19970906	1147
528	VEINS_R9	N67.2962	W026.5815	298	19970906	1355
529	VEINS_R10	N67.3482	W027.1417	239	19970906	1703
530	VEINS_R11	N67.3997	W027.3022	290	19970906	1935
531	VEINS_S12A	N66.5308	W028.0182	356	19970907	0906
532	VEINS_S11A	N66.4813	W027.3971	357	19970907	1202
533	VEINS_S10A	N66.4396	W027.2279	371	19970907	1350
534	VEINS_S9A	N66.4093	W027.1014	416	19970907	1528
535	VEINS_S8A	N66.3786	W026.5730	485	19970907	1716
536	VEINS_S7A	N66.3478	W026.4533	525	19970907	1926
537	VEINS_S6A	N66.3157	W026.3183	563	19970907	2147
538	VEINS_S5A	N66.2830	W026.1933	643	19970907	2357
539	VEINS_S4A	N66.2520	W026.0717	657	19970908	0240
540	VEINS_S3A	N66.2221	W025.5474	583	19970908	0506
541	VEINS_S2A	N66.1901	W025.4185	338	19970908	0704
542	VEINS_S1A	N66.1747	W025.3627	188	19970908	0822
543	VEINS_L1	N66.0096	W026.4791	446	19970908	1428
544	VEINS_L2	N66.0302	W026.5488	584	19970908	1602
545	ADCP_ICE	N66.0460	W027.0412	669	19970908	1802
546	VEINS_L4	N66.0700	W027.0896	618	19970908	1952
547	VEINS_L5	N66.0909	W027.1484	529	19970908	2135
548	VEINS_L6	N66.1106	W027.2091	493	19970908	2306
549	VEINS_L7	N66.1304	W027.2698	494	19970909	0048
550	VEINS_L8	N66.1498	W027.3280	498	19970909	0232
551	VEINS_L9	N66.1891	W027.4484	383	19970909	0444
552	VEINS_L10	N66.2472	W028.0232	340	19970909	0644
553	VEINS_L11	N66.3046	W028.1964	317	19970909	0838
554	VEINS_L12	N66.3623	W028.3718	327	19970909	1031
555	VEINS_L13	N66.4197	W028.5469	345	19970909	1220
556	VEINS_L14	N66.4772	W029.1226	364	19970909	1406
557	VEINS_S15A	N67.0723	W028.5888	323	19970909	1656
558	VEINS_S14A	N67.0256	W028.3928	322	19970909	1849
559	VEINS_S13A	N66.5783	W028.1966	343	19970909	2044
560	VEINS_S12A	N66.5316	W028.0006	360	19970909	2333
561	VEINS_L11	N66.3046	W028.1963	315	19970910	0652
562	VEINS_L10	N66.2472	W028.0236	342	19970910	0905

Index	Station name	Latitude	Longitude	Depth	Date	Time
563	VEINS_L9	N66.1898	W027.4505	381	19970910	1116
564	VEINS_L8	N66.1500	W027.3303	496	19970910	1256
565	VEINS_L7	N66.1298	W027.2691	498	19970910	1432
566	VEINS_L6	N66.1098	W027.2097	497	19970910	1608
567	VEINS_L5	N66.0895	W027.1492	537	19970910	1732
568	VEINS_L4	N66.0693	W027.0914	622	19970910	1913
569	ADCP_ICE	N66.0457	W027.0415	672	19970910	2056
570	VEINS_L2	N66.0315	W026.5533	600	19970910	2314
571	VEINS_E8	N65.2000	W027.3988	731	19970911	1238
572	VEINS_E7	N65.2553	W027.4729	802	19970911	1437
573	VEINS_E6	N65.3113	W027.5474	818	19970911	1635
574	VEINS_E5	N65.3670	W028.0214	835	19970911	1847
575	VEINS_E4	N65.4230	W028.0963	902	19970911	2049
576	VEINS_E3	N65.4776	W028.1717	766	19970911	2333
577	VEINS_E2	N65.5340	W028.2445	543	19970912	0223
578	VEINS_E1	N65.5898	W028.3204	459	19970912	0455

Leg 3: Isafjördur-Reykjavik 1.-13.9.1997

Index	Station name	Latitude	Longitude	Depth	Date	Time
498	VEINS_K2	N67.1498	W023.3643	397	19970902	1153
499	VEINS_K3	N67.2500	W023.4474	654	19970902	1430
500	VEINS_K4	N67.3495	W023.5315	975	19970902	1813
501	VEINS_K5	N67.4507	W024.0180	1287	19970903	0718
502	VEINS_K6	N67.5506	W024.1016	1481	19970903	1127
503	VEINS_K7	N68.0499	W024.1880	1500	19970903	1459
504	VEINS_K10	N68.1891	W025.2846	300	19970903	1935
505	VEINS_K9	N68.1418	W025.0512	729	19970903	2149
506	VEINS_K8	N68.0962	W024.4199	1279	19970904	0134
507	VEINS_H11	N68.0498	W026.1265	312	19970904	0731
508	VEINS_H10	N67.5903	W025.5602	404	19970904	0925
509	VEINS_H9	N67.5296	W025.3993	641	19970904	1128
510	VEINS_H8	N67.4723	W025.2557	1079	19970904	1329
511	VEINS_H7	N67.4149	W025.1136	1343	19970904	1600
512	VEINS_H6	N67.3565	W024.5694	1449	19970904	1851
513	VEINS_H5	N67.2999	W024.4265	1354	19970904	2210
514	VEINS_H4	N67.2426	W024.2838	1152	19970905	0208
515	VEINS_H3	N67.1854	W024.1423	877	19970905	0512
516	VEINS_H2	N67.1272	W023.5989	568	19970905	0730
517	VEINS_H1	N67.0698	W023.4574	280	19970905	0929
518	VEINS_K1	N67.0496	W023.2737	241	19970905	1100
519	VEINS_R1	N66.4800	W024.5309	579	19970905	1519
520	VEINS_R2	N66.5319	W025.0846	925	19970905	1714
521	VEINS_R2	N66.5270	W025.0955	929	19970905	1820
522	VEINS_R3	N66.5838	W025.2403	1083	19970905	2048
523	VEINS_R4	N67.0359	W025.3947	945	19970906	0009
524	VEINS_R5	N67.0877	W025.5501	835	19970906	0316
525	VEINS_R6	N67.1399	W026.1078	739	19970906	0657
526	VEINS_R7	N67.1924	W026.2628	591	19970906	0905
527	VEINS_R8	N67.2434	W026.4211	293	19970906	1147
528	VEINS_R9	N67.2962	W026.5815	298	19970906	1355
529	VEINS_R10	N67.3482	W027.1417	239	19970906	1703

Index	Station name	Latitude	Longitude	Depth	Date	Time
530	VEINS_R11	N67.3997	W027.3022	290	19970906	1935
531	VEINS_S12A	N66.5308	W028.0182	356	19970907	0906
532	VEINS_S11A	N66.4813	W027.3971	357	19970907	1202
533	VEINS_S10A	N66.4396	W027.2279	371	19970907	1350
534	VEINS_S9A	N66.4093	W027.1014	416	19970907	1528
535	VEINS_S8A	N66.3786	W026.5730	485	19970907	1716
536	VEINS_S7A	N66.3478	W026.4533	525	19970907	1926
537	VEINS_S6A	N66.3157	W026.3183	563	19970907	2147
538	VEINS_S5A	N66.2830	W026.1933	643	19970907	2357
539	VEINS_S4A	N66.2520	W026.0717	657	19970908	0240
540	VEINS_S3A	N66.2221	W025.5474	583	19970908	0506
541	VEINS_S2A	N66.1901	W025.4185	338	19970908	0704
542	VEINS_S1A	N66.1747	W025.3627	188	19970908	0822
543	VEINS_L1	N66.0096	W026.4791	446	19970908	1428
544	VEINS_L2	N66.0302	W026.5488	584	19970908	1602
545	ADCP_ICE	N66.0460	W027.0412	669	19970908	1802
546	VEINS_L4	N66.0700	W027.0896	618	19970908	1952
547	VEINS_L5	N66.0909	W027.1484	529	19970908	2135
548	VEINS_L6	N66.1106	W027.2091	493	19970908	2306
549	VEINS_L7	N66.1304	W027.2698	494	19970909	0048
550	VEINS_L8	N66.1498	W027.3280	498	19970909	0232
551	VEINS_L9	N66.1891	W027.4484	383	19970909	0444
552	VEINS_L10	N66.2472	W028.0232	340	19970909	0644
553	VEINS_L11	N66.3046	W028.1964	317	19970909	0838
554	VEINS_L12	N66.3623	W028.3718	327	19970909	1031
555	VEINS_L13	N66.4197	W028.5469	345	19970909	1220
556	VEINS_L14	N66.4772	W029.1226	364	19970909	1406
557	VEINS_S15A	N67.0723	W028.5888	323	19970909	1656
558	VEINS_S14A	N67.0256	W028.3928	322	19970909	1849
559	VEINS_S13A	N66.5783	W028.1966	343	19970909	2044
560	VEINS_S12A	N66.5316	W028.0006	360	19970909	2333
561	VEINS_L11	N66.3046	W028.1963	315	19970910	0652
562	VEINS_L10	N66.2472	W028.0236	342	19970910	0905
563	VEINS_L9	N66.1898	W027.4505	381	19970910	1116
564	VEINS_L8	N66.1500	W027.3303	496	19970910	1256
565	VEINS_L7	N66.1298	W027.2691	498	19970910	1432
566	VEINS_L6	N66.1098	W027.2097	497	19970910	1608
567	VEINS_L5	N66.0895	W027.1492	537	19970910	1732
568	VEINS_L4	N66.0693	W027.0914	622	19970910	1913
569	ADCP_ICE	N66.0457	W027.0415	672	19970910	2056
570	VEINS_L2	N66.0315	W026.5533	600	19970910	2314
571	VEINS_E8	N65.2000	W027.3988	731	19970911	1238
572	VEINS_E7	N65.2553	W027.4729	802	19970911	1437
573	VEINS_E6	N65.3113	W027.5474	818	19970911	1635
574	VEINS_E5	N65.3670	W028.0214	835	19970911	1847
575	VEINS_E4	N65.4230	W028.0963	902	19970911	2049
576	VEINS_E3	N65.4776	W028.1717	766	19970911	2333
577	VEINS_E2	N65.5340	W028.2445	543	19970912	0223
578	VEINS_E1	N65.5898	W028.3204	459	19970912	0455

2. FIELD WORK IN DENMARK STRAIT

Aranda left Reykjavik on the morning of August 18th, 1997 to commence the first transect across the northern Irminger Basin from Iceland to the shelf of Greenland (sections N and A). The cruise track and the different sections are shown in Figure 1, the station locations are seen in Figure 2 and the exact co-ordinates are given in Table 3.

After the first transect was completed Aranda sailed north, making two further sections across the Greenland slope (B and D). After this a southwest-northeast section J was taken, largely following the 1000m isobath, which was expected to coincide with the axis of the descending overflow plume. On section J the CTD observations and water sampling were augmented by XCP observations. After section J had been finished, one further cross slope section (E) was taken. XCP observations were made also on this section. Aranda then continued north into Denmark Strait, and two transects were taken across the channel from the Greenland shelf onto the Iceland shelf. Aranda entered harbour in Isafjördur on the 29th of August.

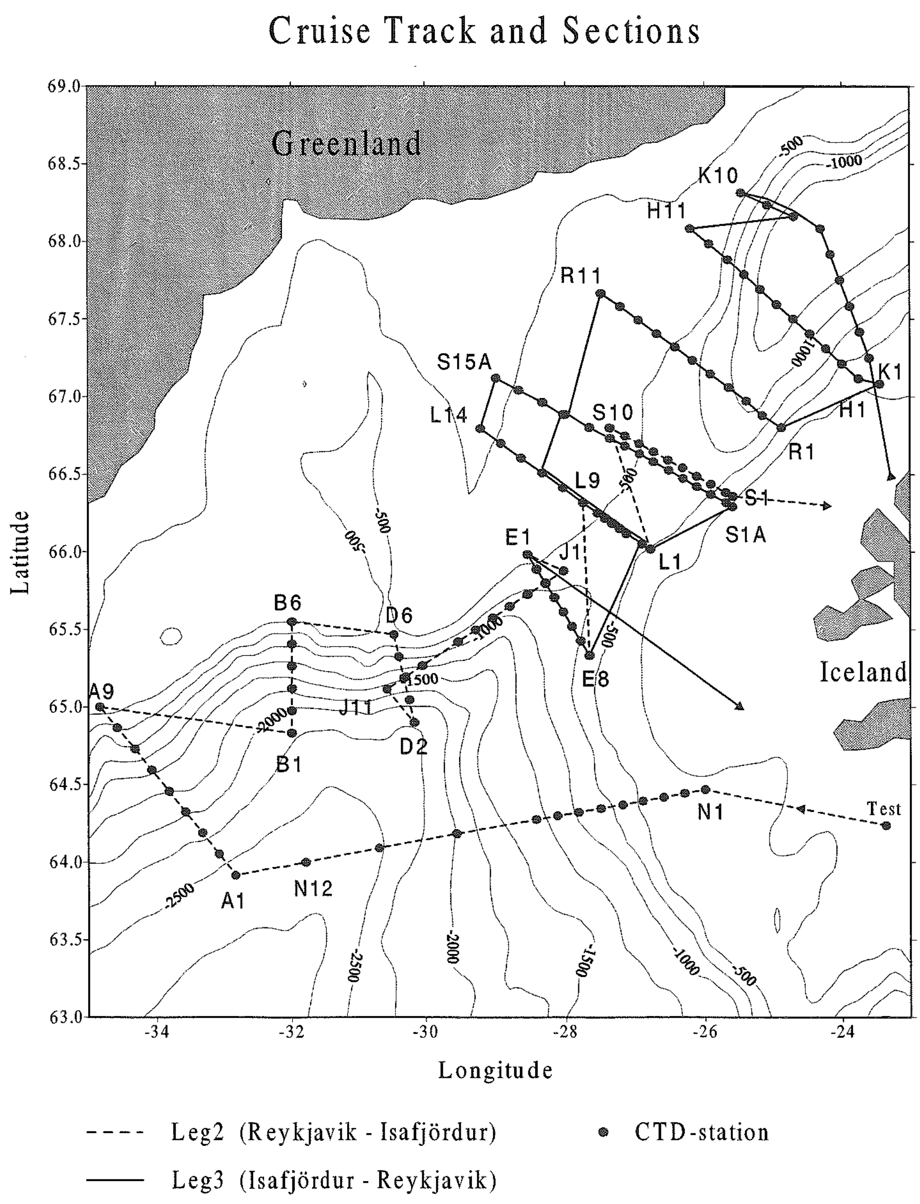

Fig. 1. The tracks of the 2nd and 3rd legs of the Aranda cruise 12/1997.

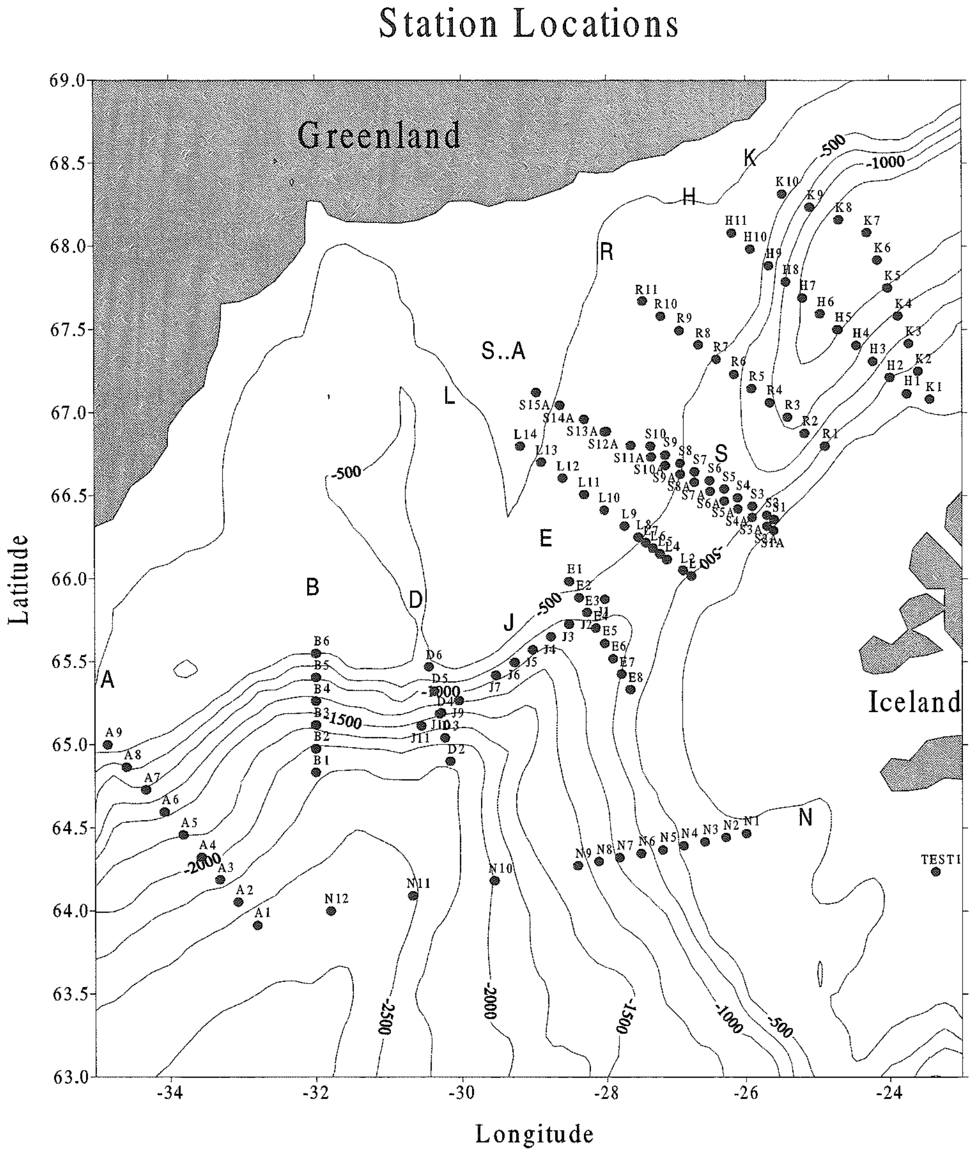

Fig. 2. Positions of the CTD stations occupied by RV Aranda in Denmark Strait in August-September 1997.

The last leg of the cruise started from Isafjördur on the 1st of September, and transect K was taken from the Iceland shelf across the Western Iceland Basin to the Greenland shelf. Aranda then continued south, and a second transect (H) was taken from the Greenland to the Iceland shelf. At the end of this transect the first station on transect K, previously cancelled because of bad weather, was occupied. A third transect (R) between the two shelves was taken, before the transects at the sill (S and L) were repeated. Because a warm water lens, originating from the Irminger Current, was observed on the Greenland shelf, the L transect was extended further westwards the second time. As Aranda returned eastwards section S was also augmented with additional western stations before section L was occupied a third time. Due to bad weather towards the end of this crossing, the easternmost L station had to be cancelled. The weather conditions improved quickly, and the cross slope section E could also be repeated. After a short study of a small-scale thermal surface front, the measurements were finished and Aranda returned to Reykjavik on the 13th of September.

3. DATA HANDLING AND CALIBRATION

The CTD observations on Aranda were made with a Sea-Bird Electronics SBE-911 plus CTD system. The CTD performed well throughout the cruise and the sensors appeared to be stable, although the conductivity sensor was somewhat noisy when strong gradients in temperature and salinity were encountered. The sensors were calibrated after the cruise by Ocean Scientific International in the UK. Salinity samples for calibrating the conductivity sensor were taken at each station. Some salinity samples were measured onboard, but most of them were analysed at the Institut für Meereskunde der Universität Hamburg. No reversing thermometers were used during the cruise.

The post calibration of the temperature sensor has been applied. However, regarding conductivity, the old calibration coefficients were used to compare the CTD with the bottle salinities. The offset between the CTD conductivity and the conductivity of the water samples was calculated using the laboratory measured salinity, the corrected CTD temperature and the CTD pressure. The difference C(bottle)-C(CTD) then becomes solely due to errors in the conductivity measurements. Following the recommendation from Sea-Bird Electronics (Application note 31) these errors were assumed to be caused by a drift in the conductivity cell, an error that should be removed by correcting the initially given 1.0 slope of the conductivity calibration, not by applying an offset between CTD and laboratory conductivity. By plotting C(bottle) against C(CTD) and fitting a linear function C(bottle)=kC(CTD) to the points, a slope k=1.00045 was obtained. This 1.00045 slope was then used instead of 1.0 in the conductivity calibration. Together with the corrected temperature, this gives an average difference between the bottle salinities and the CTD salinities well below 0.001. 24 test samples give $\Delta S=0.0004$ with standard deviation =0.0009.

In the appendix, potential temperature Θ, salinity S, and potential density σ_θ sections are shown for the different transects: A+N, B, D, E1, E2, L1, L2, L3, S1, S2, R, H, K, J and a north-south section M extending from transect K to transect A across the sill in Denmark Strait. This section comprises the deepest stations north of and at the sill, then follows section J along the slope and then continues further along the path of the plume across sections B and A. The Θ-S curves for the stations on the different sections are also shown. However, for sections, profiles and Θ-S diagrams referred to in the discussion (section 4), separate figures have been constructed and are shown in the text.

4. DISCUSSION

The contrasts between the waters north and south of the sill in Denmark Strait are seen by comparing potential temperature, salinity and potential density sections from transect A+N across the Irminger Basin and transect H across the West Iceland Basin (Fig. 3).

On transect A+N, the warm, saline water of the Irminger Current is seen to circulate along the Iceland continental slope and then return southward along the Greenland continental slope to the west. The current bifurcates at the strait and one part enters the Iceland Sea and flows northward along the Iceland continental slope, where it is seen as a warm, saline wedge on the easternmost H stations.

In the central Irminger Sea the isolines dome upwards and a salinity minimum (S<34.90) is present around 800m. The temperature of the minimum is slightly below 4 °C. The minimum extends to a shallower depth at station A3, where the isotherms and isopycnals also rise towards the surface. This suggests that the salinity minimum layer is a remnant of local winter convection, which then would reach almost 1000m. This agrees with the depth of the winter mixed layer in the Irminger Sea shown by Woods (1984, Figure 9.4). It is interesting that the Transient Tracers in the Ocean (TTO) salinity section across the Irminger Sea taken occupied in 1981 and shown by Dickson & Brown (1994), also indicates a similar "chimney" at the same position. The salinities were, however, higher that year.

A second salinity minimum (S<34.86) is observed near 2000m. Its temperature is just below 3 °C indicating advected, newly-ventilated Labrador Sea Water (LSW) (Talley & McCartney, 1982). Its transit time from the Labrador Sea to the Irminger Sea has been found to be surprisingly small (Sy & al., 1997). The two minima are also conspicuous in the Θ-S curves (Fig. 4).

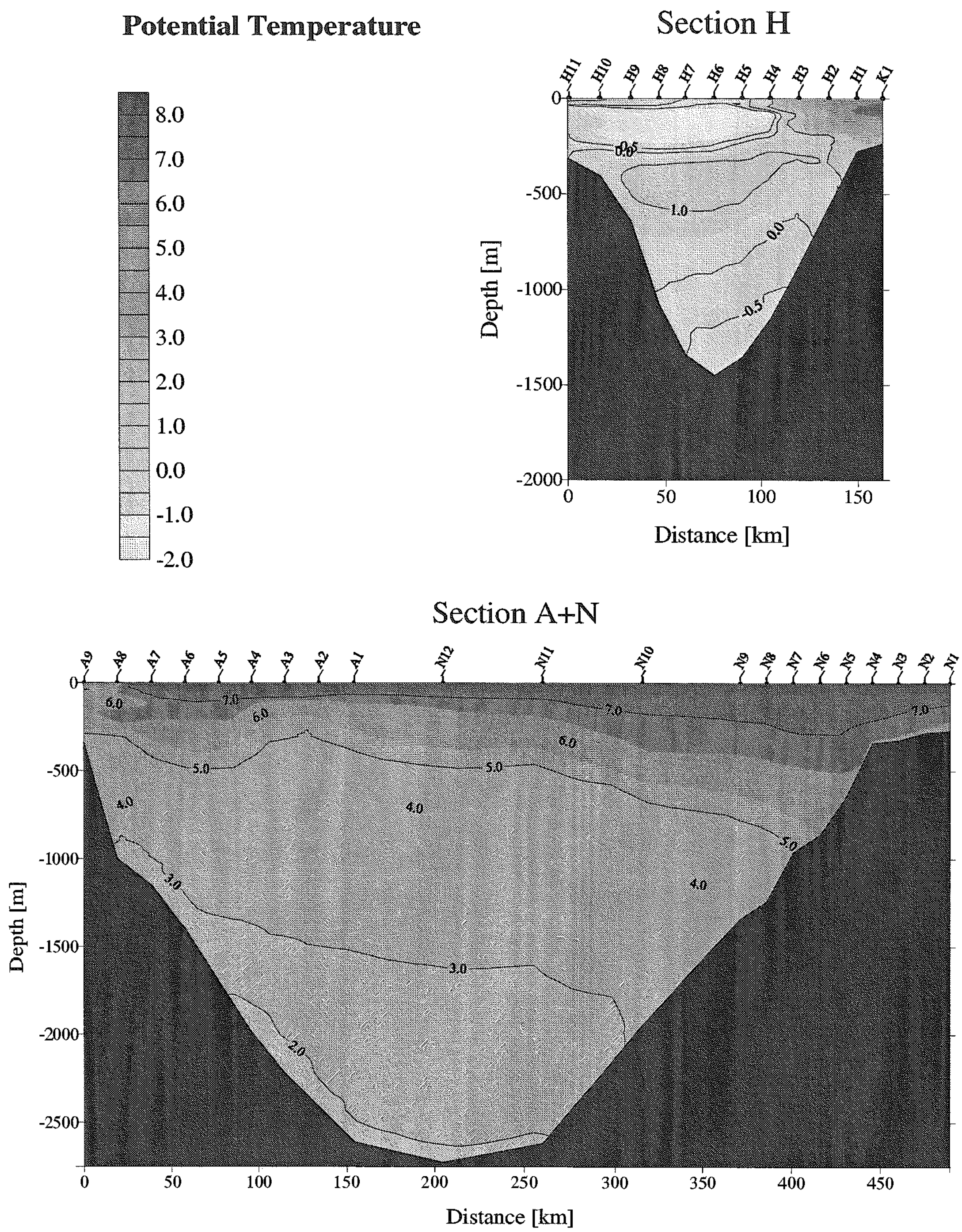

Fig. 3a. The potential temperature Θ distributions between Greenland and Iceland on transect H across the Western Iceland Basin (top), and on transect A+N across the Irminger Basin (bottom).

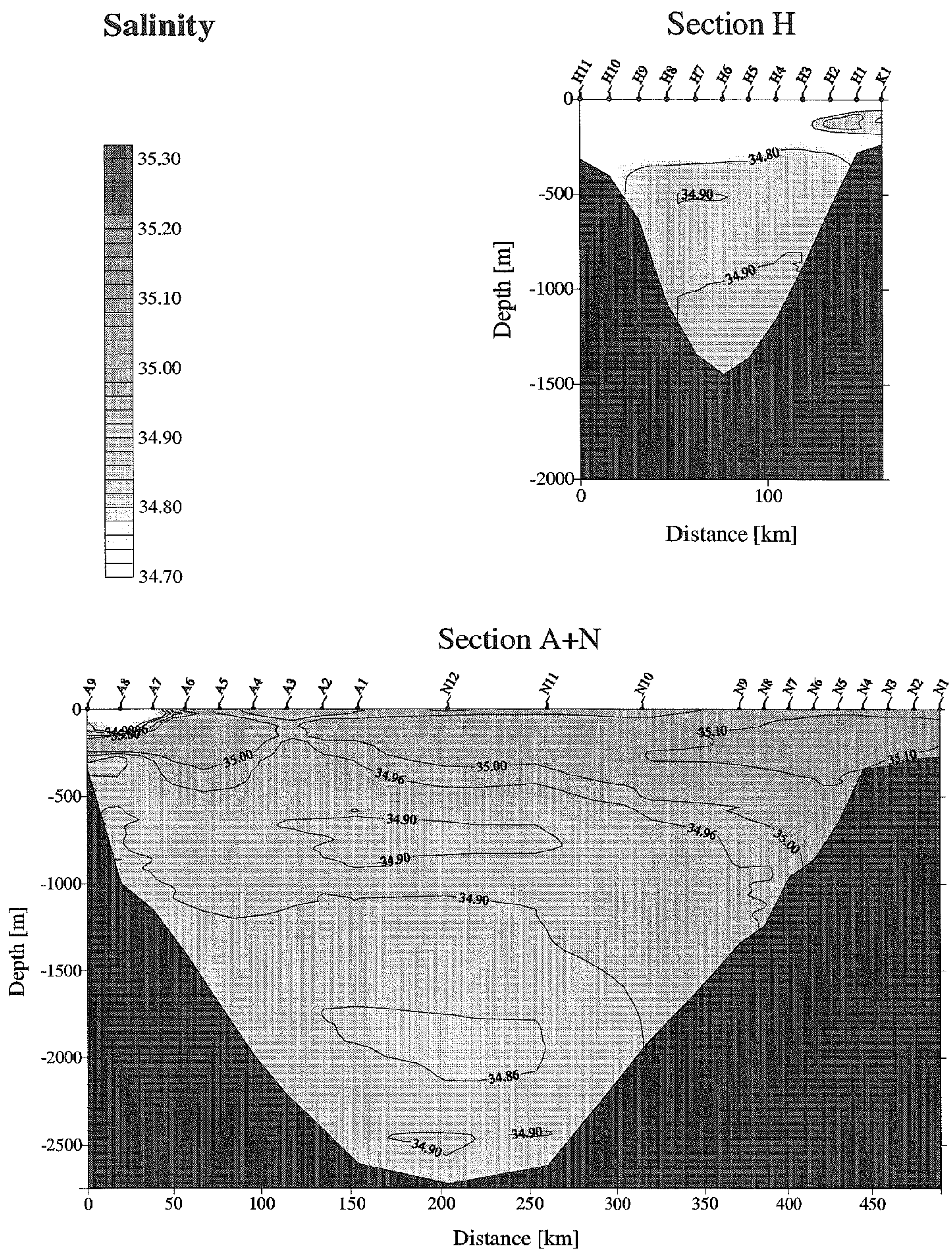

Fig. 3b. The salinity S distribution between Greenland and Iceland on transect H across the Western Iceland Basin (top), and on transect A+N across the Irminger Basin (bottom).

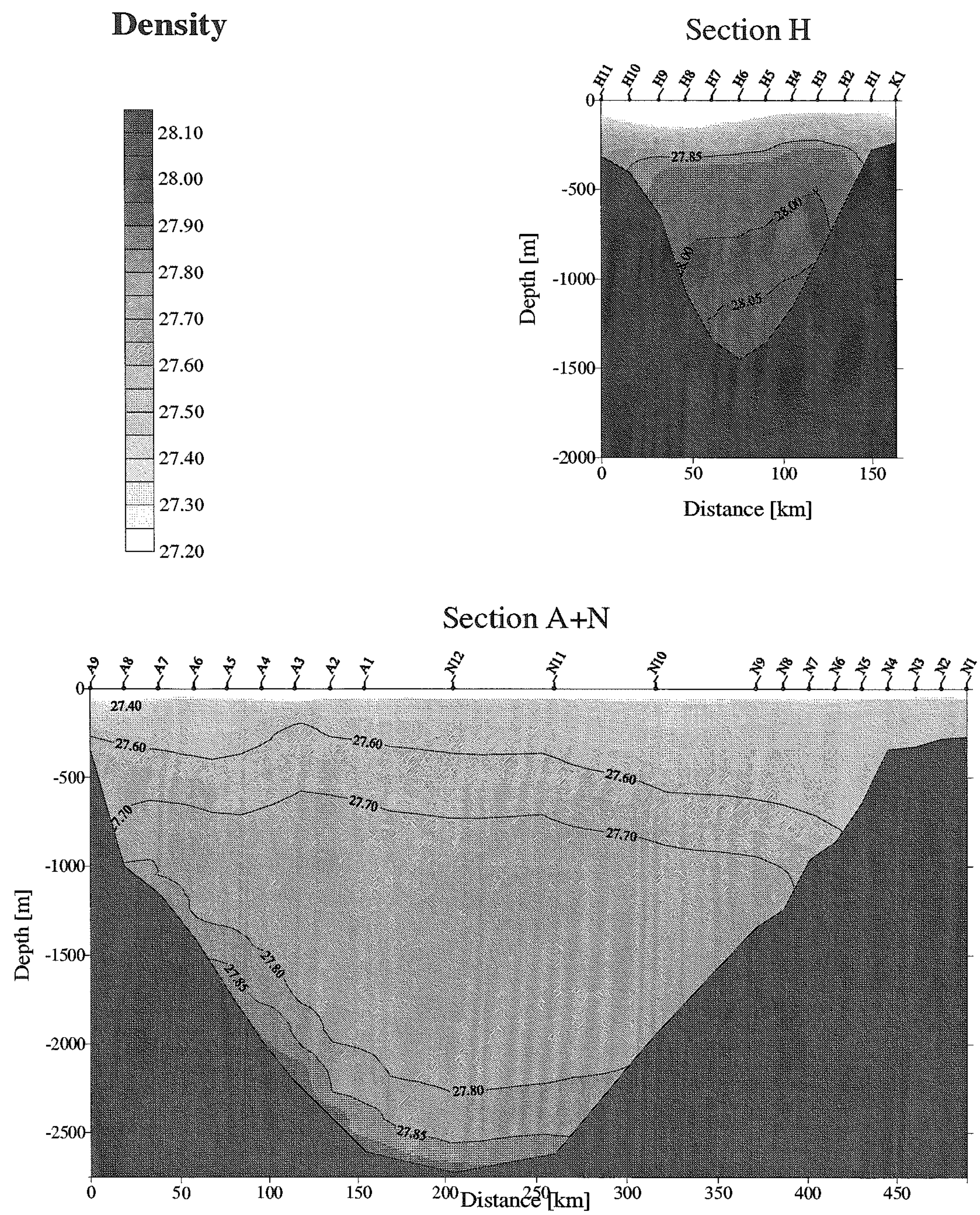

Fig. 3c. The potential density σ_θ distribution between Greenland and Iceland on transect H across the Western Iceland Basin (top), and on transect A+N across the Irminger Basin (bottom).

Below the LSW a weak temperature and salinity maximum is found. It is seen most clearly on the Θ-S curves from the deep eastern part of section N. It is due to the presence of Northeast Atlantic Deep Water (NEADW), which enters the Irminger Basin through the Gibbs Fracture Zone but is ultimately formed from the entraining Iceland-Scotland overflow (Swift, 1984). On the Greenland slope below 1500m and at the deepest stations of the transect, a cold ($\Theta<2$ °C, occasionally below 1.5 °C), and dense ($\sigma_\theta>27.85$) bottom layer is observed. This is the Denmark Strait Overflow Water (DSOW) originating from north of the sill.

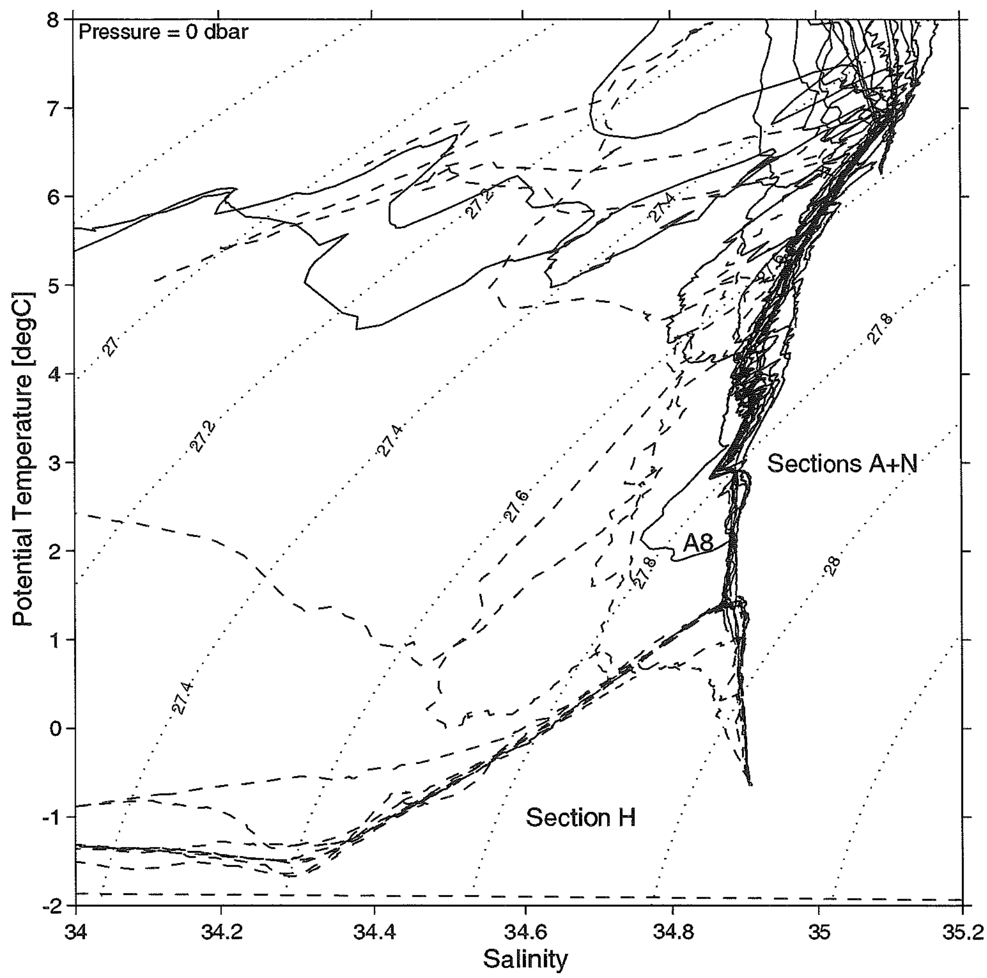

Fig. 4. Θ-S diagram showing the stations on transect H (dashed) and on section A+N (full lines).

In the Iceland Sea, away from the Iceland shelf and slope, the cold, low-salinity polar water of the East Greenland Current is present in the upper layers on most of section K (Fig. 3). The temperature minimum is close to freezing, and the salinity at the temperature minimum is around 34.3, as is evident from the Θ-S diagram in Figure 4. This is close to the salinity of the winter mixed layer recently observed in the Eurasian Basin of the Arctic Ocean (Steele & Boyd, 1998). South of the sill, the low salinity upper layer is only seen over the Greenland shelf far to the west (Fig. 3).

Below the cold upper layer, a temperature maximum is found at about 500m across the section. The temperature is below 2 °C and its salinity is about 34.9. These comparatively low values show that it derives from the north, either originating from the Atlantic Water recirculating in Fram Strait (Bourke & al., 1988), or from the Atlantic Layer of the Arctic Ocean (Rudels, 1987). The isopycnals slope downwards toward Greenland, consistent with a southward baroclinic flow of the East Greenland Current (Fig. 3). The shape of the Θ-S curves, especially the temperature minimum and the thermocline, suggests the Arctic Ocean as a source, but the temperature of the maximum is high compared to the Arctic Ocean and some warmer water from Fram Strait must be present. Surprisingly, the Θ-S curves are smooth and do not show indications of recent mixing and interleaving (Fig. 4).

The intermediate temperature maximum is absent close to Iceland, and the deep isopycnals become shallower at the Iceland continental slope, suggesting a deep boundary flow toward the north. This implies that the water masses of the East Greenland Current in the density range of the temperature maximum cross the sill into the Irminger Basin, contributing to the DSOW, while the densest part of the East Greenland Current largely recirculates eastward north of Iceland, eventually to enter the Norwegian Sea. Such recirculation must, however, lie deeper than 800m, because current observations at the Iceland continental slope indicate a westward flow extending at least down to this level (Jónsson, 1997).

A salinity minimum is observed between the upper, warm Irminger Current water and the recirculating deeper waters; the slope of the Θ-S curves between this minimum and the deep water is stable both in temperature and in salinity (Fig. 5).

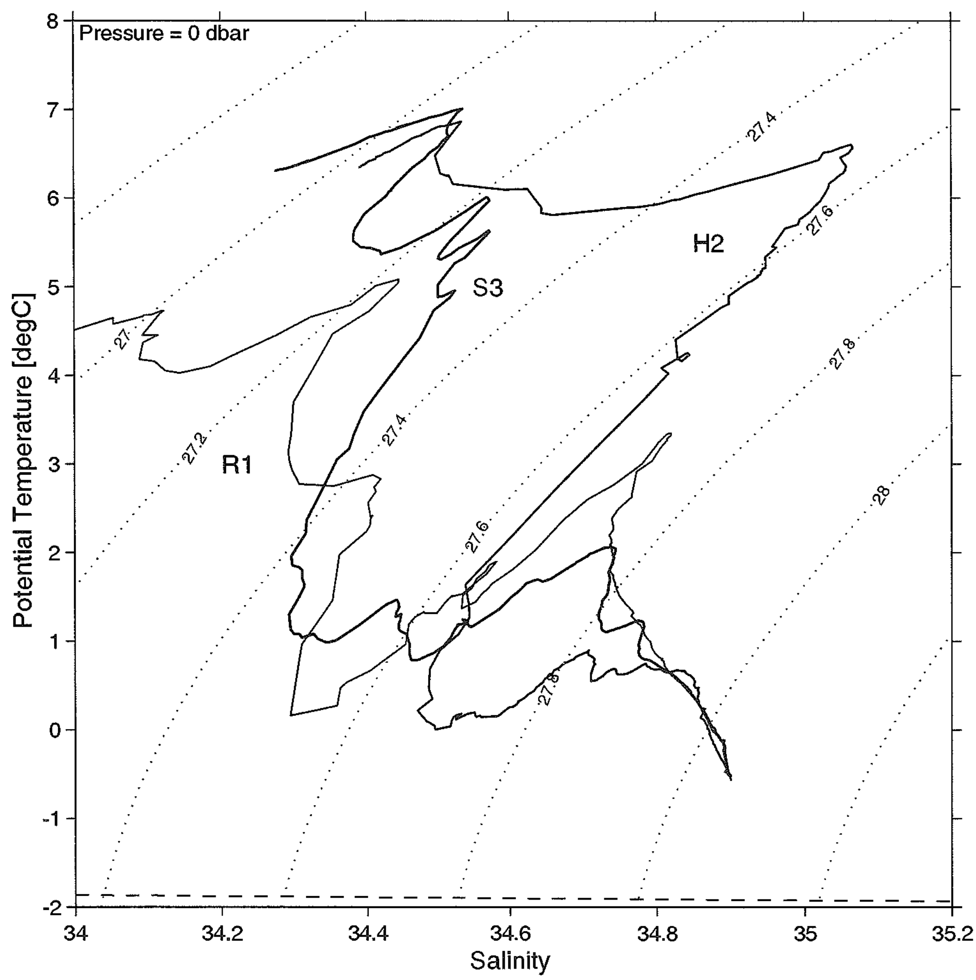

Fig. 5. Θ-S curves from stations R1, H2 and S3 showing the intermediate salinity minimum and the stable-stable stratification at the continental slope north of Iceland.

There is no obvious advective source for such a water mass, and it is most likely formed by mixing between the Atlantic Water of the Irminger Current and waters from the thermocline and the temperature maximum of the East Greenland Current as they meet north of the sill. It is interesting that this mixing leads to a similar Θ-S slope as e.g. that of the upper Polar Deep Water formed by entraining boundary plumes in the Arctic Ocean (Rudels & al., 1994).

A meridional section across the sill from the Iceland Sea to the Irminger Sea (Fig. 6) shows the sharp front between the water masses between the two basins and the descending cold and dense overflow plume. Profiles of potential temperature, salinity and potential density from stations south of the sill (Fig. 7), reveal that the DSOW plume is stratified and appears to consist of a homogenous deeper part about 50-100m thick, with a salinity around 34.9 and temperatures between 0 °C and 1 °C. This lower part is covered by a low salinity lid, which occasionally also exhibits a weak temperature minimum. The density of the lid is close to that of the LSW, but its low salinity shows that it cannot be created by entrainment of LSW, or any other ambient water mass, into the plume. The lid is also observed at levels above the LSW where the temperature and salinity of the ambient water are still higher.

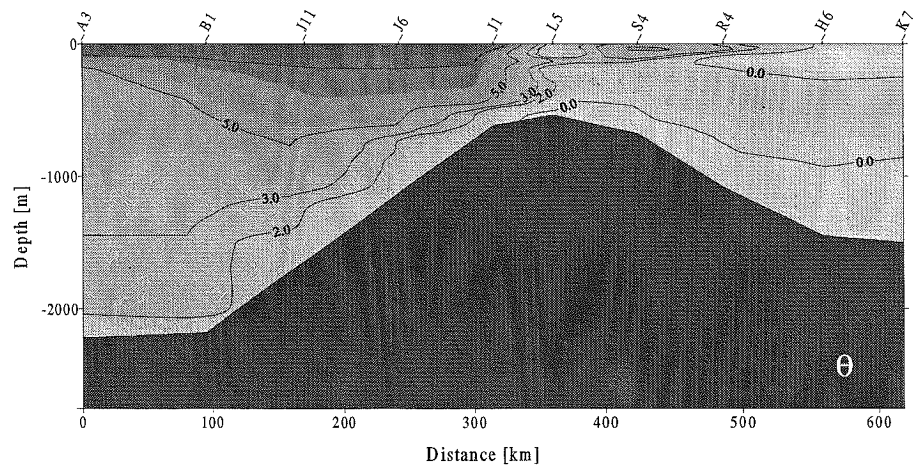

Fig. 6a. North-south section of potential temperature Θ comprising the deepest stations north of Denmark Strait and at the sill. South of the sill the section follows section J and then the path of the overflow plume as it crosses sections D, B and A.

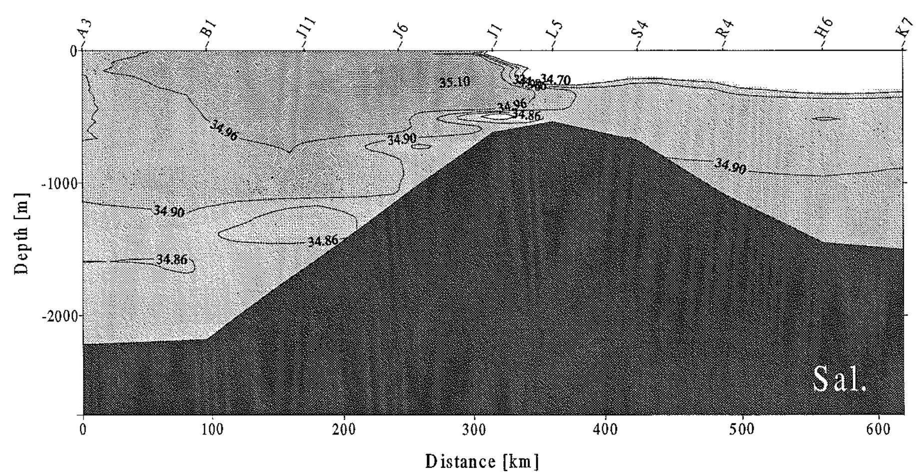

Fig. 6b. North-south section of salinity comprising the deepest stations north of Denmark Strait and at the sill. South of the sill the section follows section J and then the path of the overflow plume as it crosses sections D, B and A.

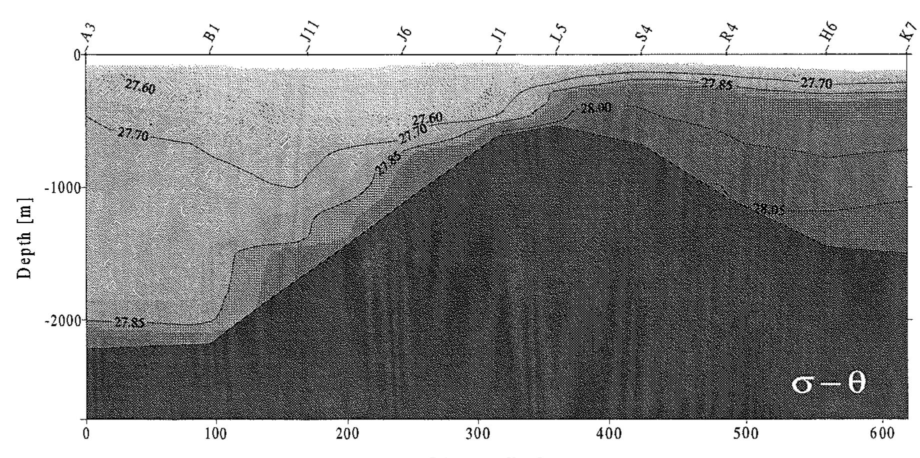

Fig. 6c. North-south section of potential density σ_θ comprising the deepest stations north of Denmark Strait and at the sill. South of the sill the section follows section J and then the path of the overflow plume as it crosses sections D, B and A.

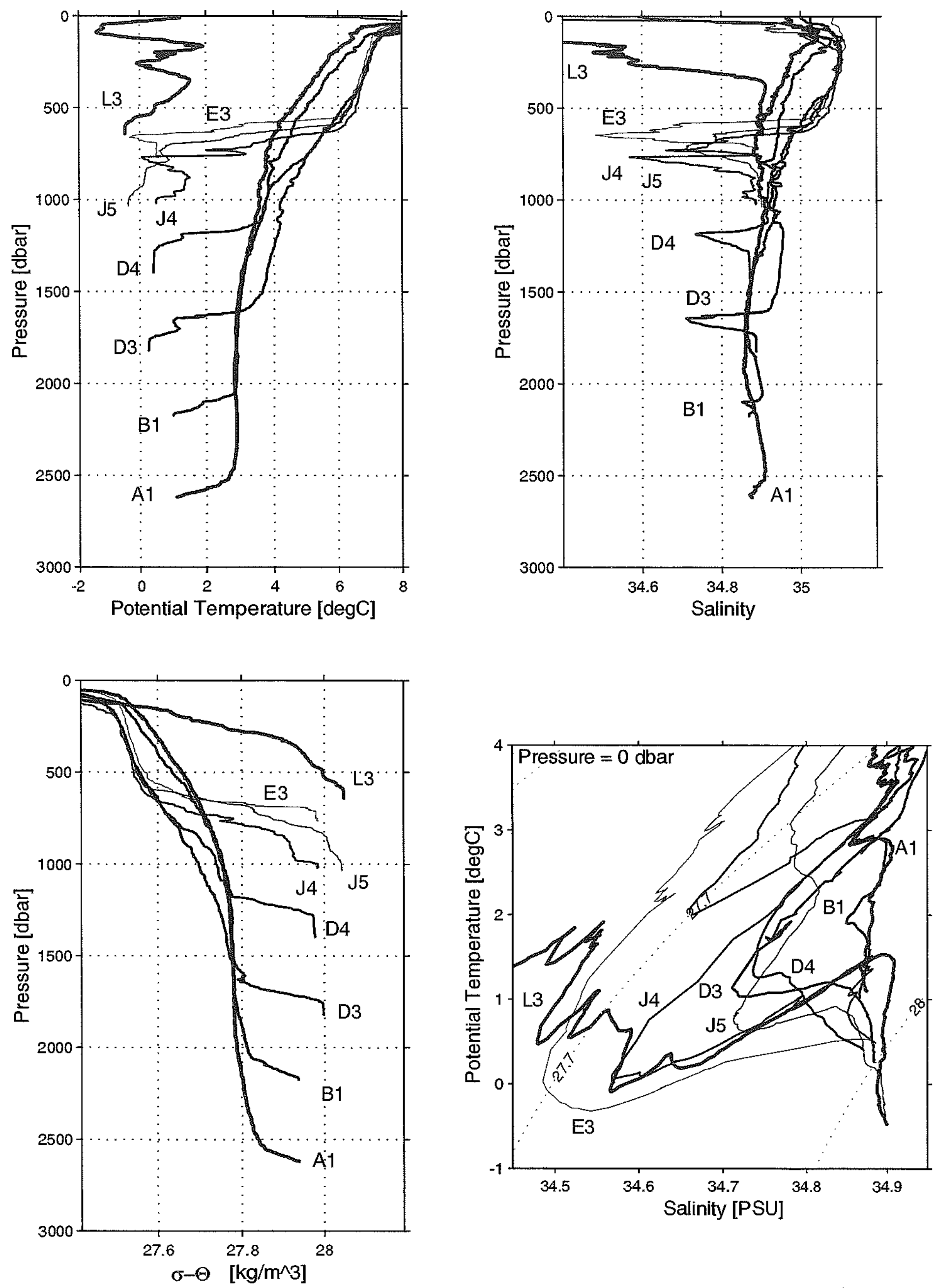

Fig. 7. Profiles of potential temperature Θ, salinity S and potential density σ_θ and Θ-S curves from stations L3, E3, J4, J5, D4, D3, B1, A1 along the path of the descending overflow plume showing the presence of the low salinity lid.

The properties of the lid resemble those of the thermocline above the temperature maximum north of the sill (Fig. 3). The characteristics of the lower, homogenous part of the plume are somewhat different from those of the temperature maximum. However, if waters of the thermocline, of the temperature maximum, and of the underlying, colder intermediate layer cross the sill and mix internally as they sink down the slope, the stratification within the plume would gradually become weaker, and Θ-S characteristics similar to those encountered in the plume, in the homogenous part as well as in the lid, would be created. The mixing would then not involve entrainment of ambient water, and thus not be generated by interfacial stress and instabilities between the plume and the surrounding waters. The energy supply for the mixing must either arise from turbulence, generated by bottom stress, or from instabilities associated with a velocity shear within the plume. The homogenous, lower part of the plume suggests the former. A progressive homogenisation of the plume retains the density difference between the upper part of the plume (the low salinity lid) and the ambient water by increasing the density of the lid and lowering the density of the homogenous part. The entire plume could sink down the slope without its upper part becoming "shaved off".

That the overflow plume reaches 1500-2000m without substantial entrainment is surprising and contrary to the view that most of the entrainment into boundary plumes occurs at the beginning of their descent down the continental slope (Dickson & al., 1990; Dickson & Brown, 1994; Price & O'Neil Baringer, 1994). The 1997 Aranda observations might represent a special situation of the Denmark Strait overflow. However, the presence of low salinity water, the Polar Intermediate Water, at the sill and in the upper part of the overflow plume has been observed on several previous occasions (Malmberg, 1972), and the possibility that the overflow plume attains its downstream characteristics by internal mixing between several different, contributing overflow waters, not by entrainment, has been proposed earlier (Müller, 1978).

The formation of the low salinity lid could be connected with the recirculation of the Irminger Current at the sill. As the warm Irminger Current water returns towards the south, it intrudes into the East Greenland Current within the density range of the thermocline. The East Greenland Current becomes separated into a low-density upper part and a dense lower part (Fig. 8).

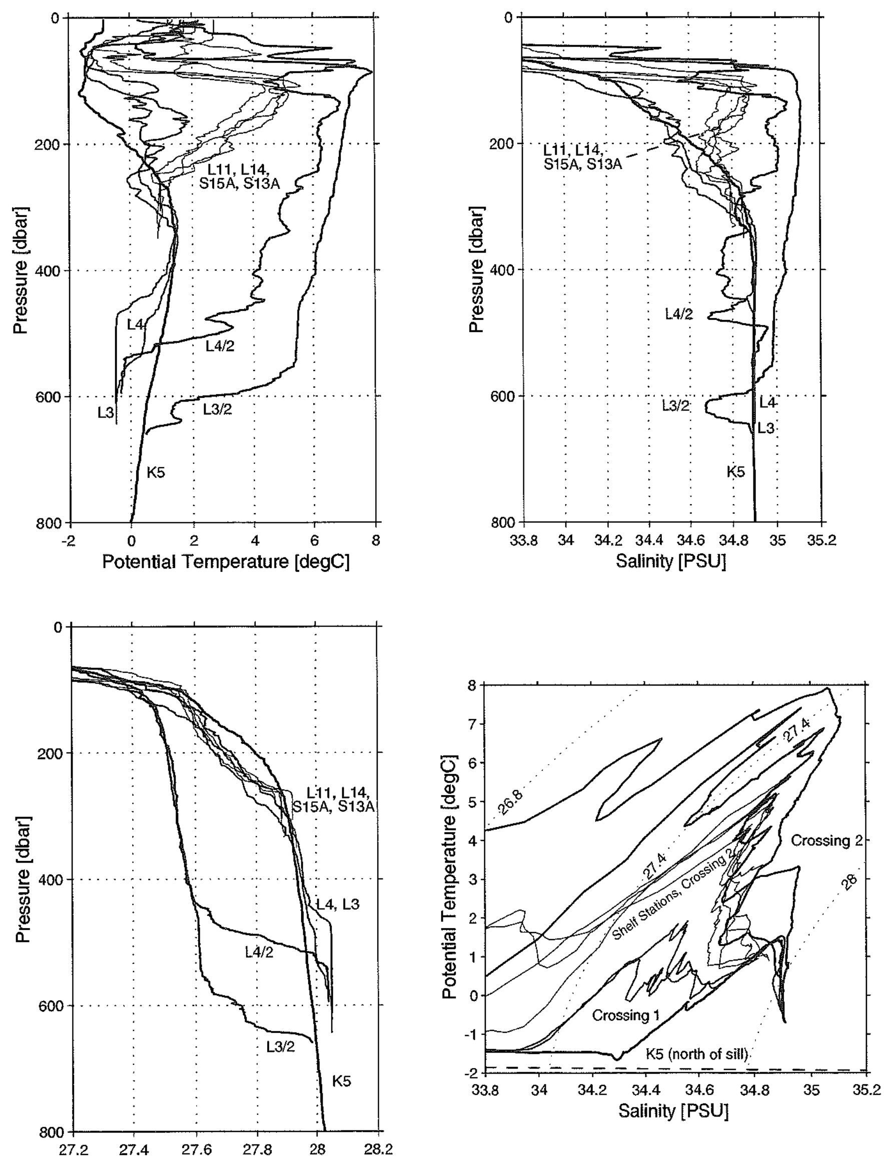

Fig. 8. Profiles of potential temperature Θ, salinity S and potential density σ_θ and Θ-S curves from selected stations from the two crossings at the sill along transect L, which show the intruding Irminger Current water. The upstream conditions are represented by station K5.

The dense part supplies the North Atlantic Deep Water, while the low-density part enters the Labrador Sea and Baffin Bay to eventually influence convection in the Labrador Sea. This splitting could actually be viewed as the final stage of the separation of the Atlantic Water entering the Arctic Mediterranean Sea into a low-salinity and a high-salinity part caused by the thermohaline processes active in the Arctic Mediterranean.

Because of its comparatively low density, the Irminger Current water reaches far west onto the Greenland shelf and splits the East Greenland Current into a high and a low density part, separated by a temperature maximum, also over the shelf. As the shelf narrows toward the south, the dense part of the East Greenland Current may cross the shelf break and sink down the slope beneath the warmer Irminger Current water flowing along the slope. It could then join, and augment, the main overflow plume, adding a comparably low density, upper fraction south of the sill, which has not passed through the deepest part of the channel. An example of this is seen on station A9 (Fig. 4). A schematic, giving a simplified picture of the circulation at the sill, is shown in Figure 9.

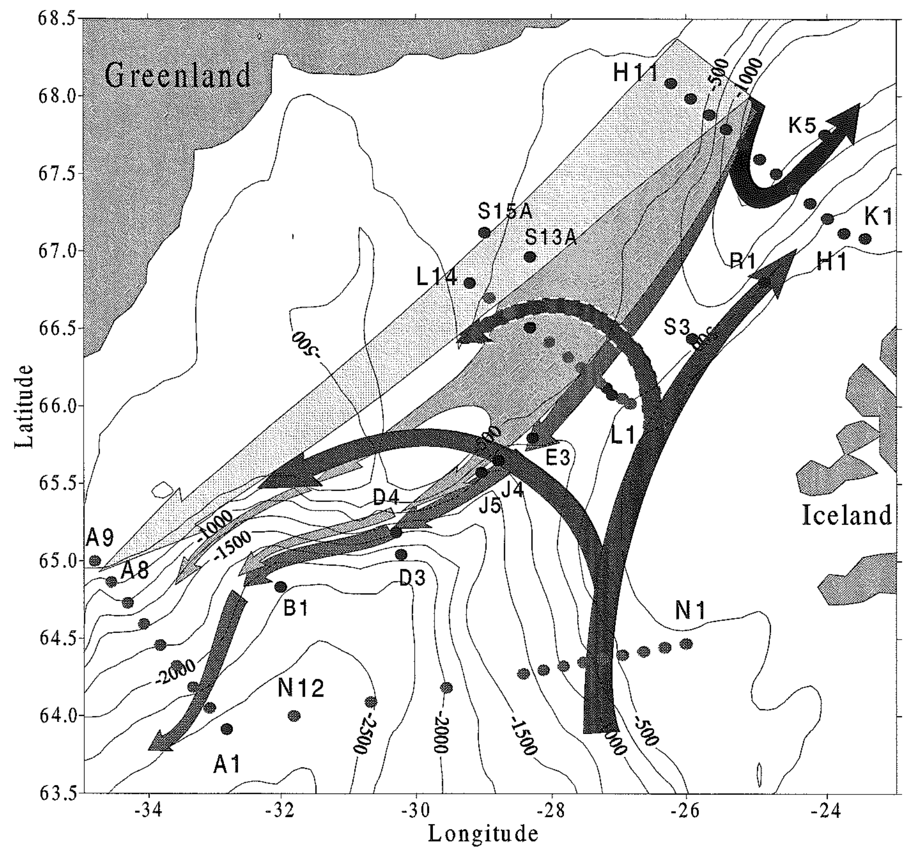

Fig. 9. Schematics showing the inferred circulation. The upper part of the East Greenland Current (faint grey), the recirculating deep water (black), the overflow plume (grey) with its low salinity lid (light grey) and less dense upper core (light grey), together with the IC with two possible positions of the westward circulating branch (dark grey). Positions of sections and stations are indicated.

The repeated sections at the sill show, as has been previously well known, that the conditions at the sill are very variable (Ross, 1978, 1984). The difference between the first and second crossings at sections L and S indicated a change from an almost complete dominance of Arctic water masses, with the Irminger Current water only present at the stations closest to Iceland, to a situation in which the warm Irminger Current water occupied most of the intermediate depth of the cross sections. However, eddies or bands of colder Arctic water were observed within the warm Irminger Current water. (Fig. 10).

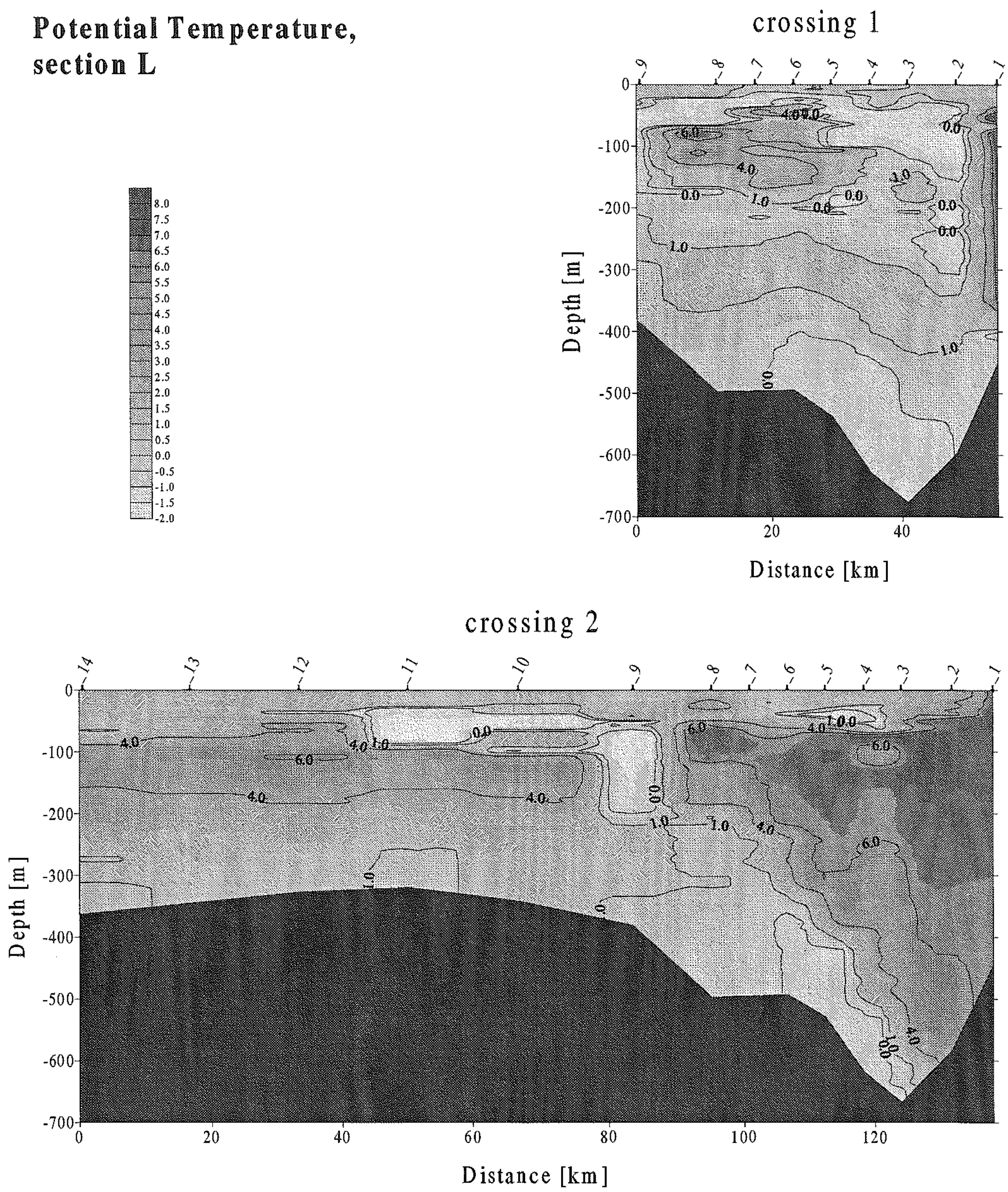

Fig. 10a. The potential temperature Θ distributions on the two crossings L1 and L2 at the sill taken at an interval of 12 days. The second crossing is extended further west onto the Greenland shelf.

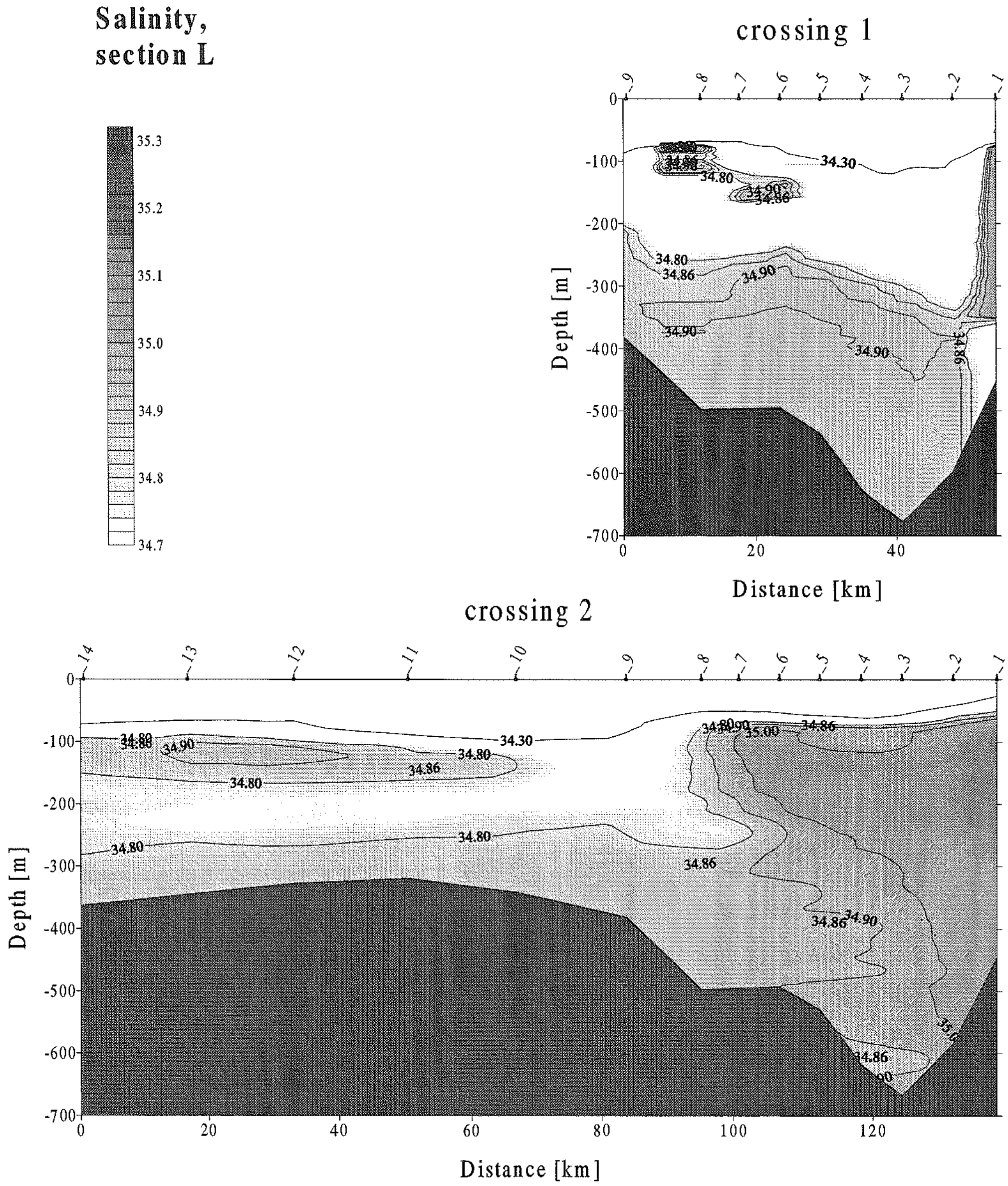

Fig. 10b. The salinity S distribution on the two crossings L1 and L2 at the sill taken at an interval of 12 days. The second crossing is extended further west onto the Greenland shelf.

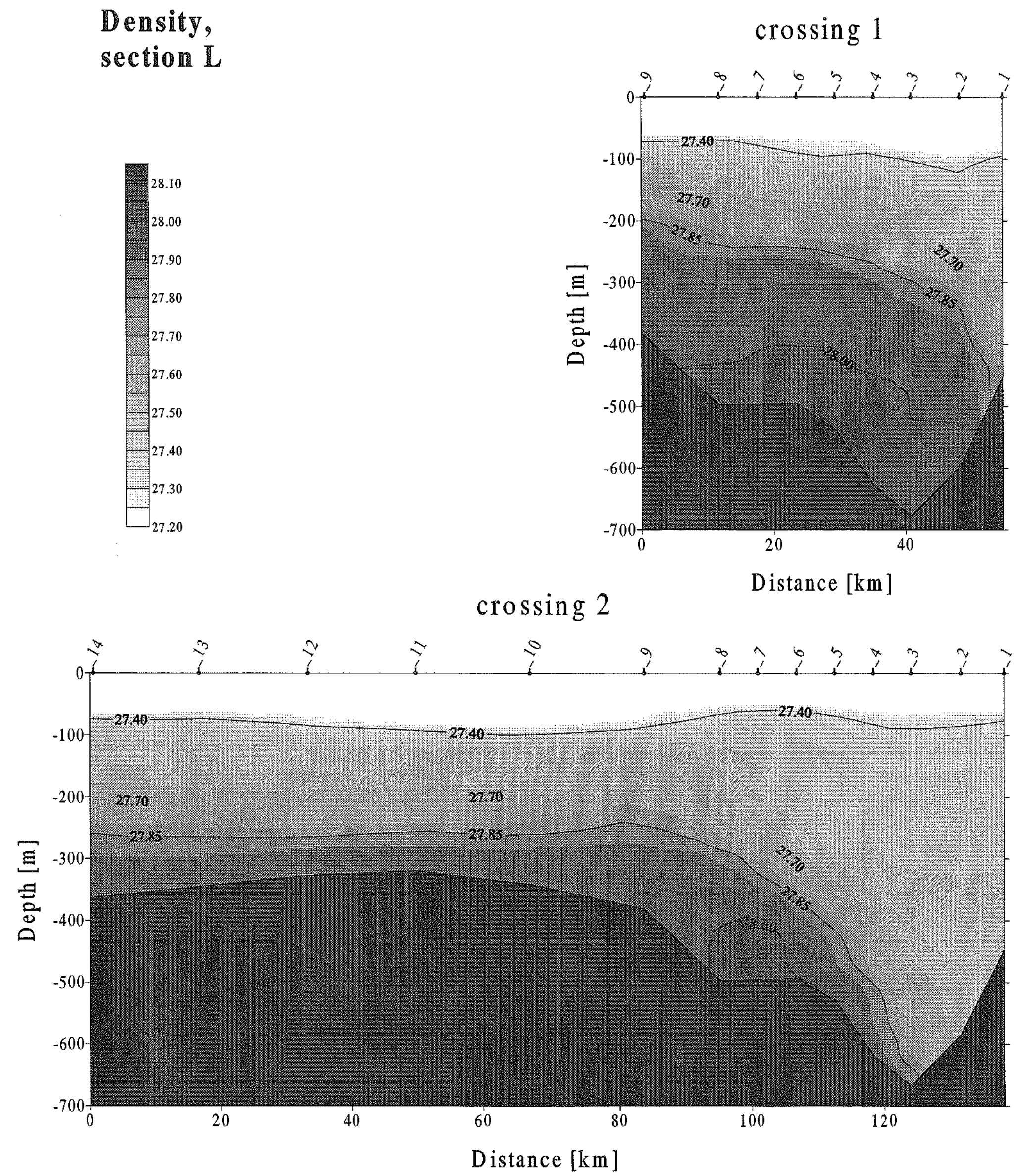

Fig. 10c. The potential density σ_θ distribution on the two crossings L1 and L2 at the sill taken at an interval of 12 days. The second crossing is extended further to the west onto the Greenland shelf.

During the same time, the area occupied by dense deep and bottom water diminished and shifted westwards. The Irminger Current water extended far to the west over the Greenland shelf, where it would eventually be carried southward by the East Greenland Current.

In addition to the short-term variability at the sill, long periodic changes in the overflow characteristics have also been observed. Dickson & al. (1999) noticed that the temperature of the overflow plume in winter 1997 was the highest recorded (>2.40 °C), and the plume was located higher up on the continental slope than "normal". They assumed that the high temperatures were associated with the Atlantic Water recirculating in Fram Strait, which because of the then high NAO (North Atlantic Oscillation) index, had been exposed to less severe cooling in the Norwegian Sea. The NAO index gives the difference between the atmospheric pressure over the Azores and over Iceland. Large differences (high index) indicate warm, windy and wet periods over the Nordic Seas. Because of a drop in the NAO index in 1995, the Atlantic Water temperatures in Fram Strait again became lower. Assuming a transit time of 3 years from Fram Strait to Denmark Strait, Dickson & al. (1999) expect to observe a decrease in overflow temperatures, perhaps already in the winter 1998. The Aranda observations show that the temperature was already lower in autumn 1997.

The temperature maximum in the water column north of the sill did not reveal temperatures as high as those expected for Atlantic Water recirculating in Fram Strait, nor the lower temperatures of the water of the Atlantic Layer in the Arctic Ocean. The Θ-S curves lie between the characteristics of these two source waters, and the smoothness of the Θ-S curves suggests that a rather complete mixing has occurred before these water masses reach Denmark Strait. Such complete mixing may not always be the case, since the maximum temperatures of the Atlantic Water are often higher and the profiles more irregular than was observed in 1997 (Rudels & al., 1998). The salinity and density of the deepest layers have also become lower compared to previous observations (Buch & al., 1996). The salinity is practically constant with depth, and the density increase is almost exclusively due to the decrease in temperature. No such obvious signs of Arctic Ocean Deep Water as were observed by Buch & al. (1996) are now present. These differences and the year-to-year variability documented by Buch & al. (1996) may be due to the path of the East Greenland Current as it crosses the Greenland and Jan Mayen Fracture Zones. Parts of the current may enter the Boreas Basin and the Greenland Sea Basin, and water of different characteristics from these basins may join the part of the East Greenland Current that by-passes the Greenland Sea. The depths at which such exchanges occur would be conditioned by the density of the water formed by winter convection in the Greenland Sea and in the Boreas Basin in different years.

Acknowledgements

We wish to thank the captains and crews on RV Aranda, and the other participants on the cruise for their support and co-operation. The present work was supported by the European Commission MAST III Programme VEINS, through contract MAS3-CT96-0070.

REFERENCES

Anonymous, 1997: Cruise 12/1997 VEINS-Nordic WOCE, Cruise Report. - Finnish Institute of Marine Research, 12 + 11 pp.

Bourke, R.H., Weigel, A.M. & Paquette, R.G. 1988: The westward turning branch of the West Spitsbergen Current. - J. Geophys. Res. 93:14065-14077.

Buch, E., Malmberg, S.-A. & Kristmannsson, S.S. 1996: Arctic Ocean deep water masses in the western Iceland Sea. - J Geophys. Res., 101:11965-11973.

Dickson, R.R., Gmitrowicz, E.M. & Watson, A.J. 1990: Deep water renewal in the northern North Atlantic. - Nature, 344:848-850.

Dickson, R.R & Brown, J. 1994: The production of North Atlantic Deep Water: Sources, rates and pathways. - J. Geophys. Res., 99:12319-12341.

Dickson, R.R., Meincke, J., Vassie, J., Jungclaus, J. & Østerhus, S., 1999: Possible predictability in overflow from the Denmark Strait. - Nature, 397:243-246.

Jónsson, S. 1997: The East Greenland Current from Fram Strait to Denmark Strait. - VEINS, Report on the 1st Workpackage Workshop, November 24 1997, Hamburg.

Malmberg, S.A. 1972: Intermediate Polar Water in the Denmark Strait - "overflow" August 1971. - ICES CM 1972/C:6.

Müller, T.J. 1978. T-S characteristics and water masses during Overflow 73. - ICES CM 1978/C:10.

Price, J.F. & O'Neil Baringer, M. 1994: Outflows and deep water production by marginal seas. - Progr. in Oceanogr., 33:161-200.

Ross, C.K. 1978: Overflow variability in Denmark Strait. - ICES CM 1978/C21, Int. Council. for the Explor. of the Sea, Copenhagen.

Ross, C.K. 1984: Temperature-salinity characteristics of the "overflow" water in Denmark Strait during "Overflow 73".- Rapp. Proc. Verb. Reun. Explor. Mer., 185:111-119.

Rudels, B. 1987: On the mass balance of the Polar Ocean, with special emphasis on the Fram Strait. - Norsk Polarinstitutt Skrifter 188. 53 pp.

Rudels, B., Jones, E.P., Anderson, L.G. & Kattner, G. 1994: On the intermediate depth waters of the Arctic Ocean. - In: "The role of the Polar Oceans in Shaping the Global Climate." O.M. Johannessen, R.D. Muench & J.E. Overland, eds, Geophysical Monographs 85, American Geophysical Union, Washington, 33-46.

Rudels, B., Quadfasel, D. & Friedrich, H.J. 1998: The Arctic Ocean Deep Water in the Greenland-Scotland Overflow. - ICES Cooperative Research Report No. 225:172-194.

Steele, M. & Boyd, T. 1998: Retreat of the cold halocline layer in the Arctic Ocean. - J. Geophys. Res. 103:10419-10435.

Swift, J.H. 1984: The circulation of the Denmark Strait and the Iceland-Scotland overflow waters in the - North Atlantic Deep-Sea Res. 31:1339-1355.

Sy, A., Rhein, M., Lazier, J., Koltermann, K.-P., Meincke, J., Putzka, A. & Bersch, M. 1997: Surprisingly rapid spreading of newly formed intermediate waters across the North Atlantic Ocean. - Nature 386:675-679.

Talley, L.D. & McCartney, M.S. 1982: Distribution and circulation of Labrador Sea Water. - J. Phys. Oceanogr. 12:1189-1205.

Woods, J.D. 1984: The upper ocean and air-sea interaction in global climate. - In:"The Global Climate", J.T. Houghton, ed., Cambridge University Press, Cambridge, 141-187.

Worthington, L.V. 1976: On the North Atlantic Circulation. - Johns Hopkins Oceanographic Studies No. 6., The Hopkins University Press, 110 pp.

HYDROGRAPHIC OBSERVATIONS IN DENMARK STRAIT ON THE VEINS EXPEDITION WITH RV ARANDA IN AUGUST-SEPTEMBER 1997

APPENDIX A

Section A - N

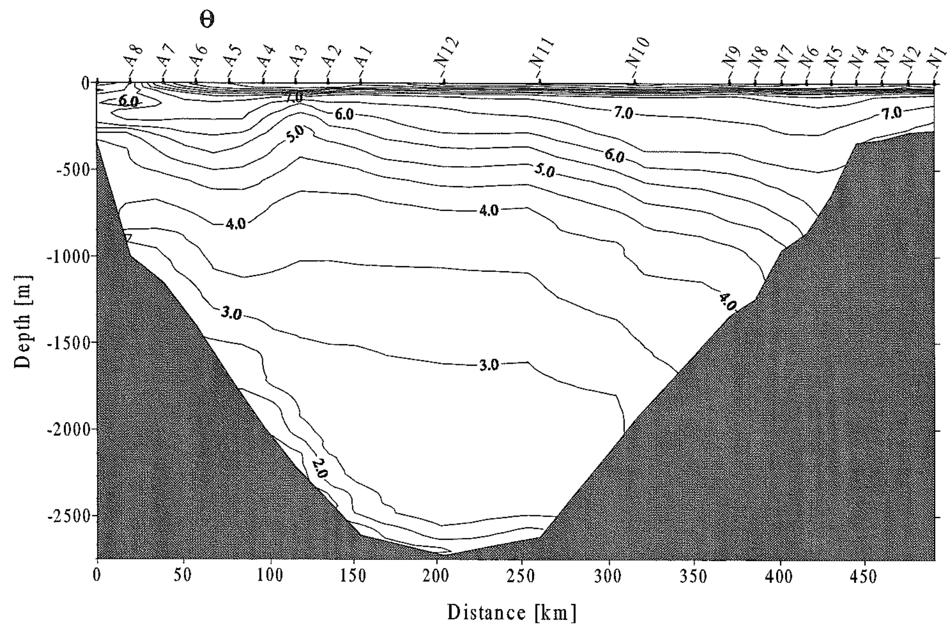
θ
A8
A7
A6
A5
A4
A3
A2
A1
N12
N11
N10
N9
N8
N7
N6
N5
N4
N3
N2
N1
6.0
7.0
6.0
5.0
7.0
6.0
5.0
7.0
4.0
4.0
3.0
4.0
3.0
2.0
0
-500
-1000
-1500
-2000
-2500
Depth [m]
0
50
100
150
200
250
300
350
400
450
Distance [km]

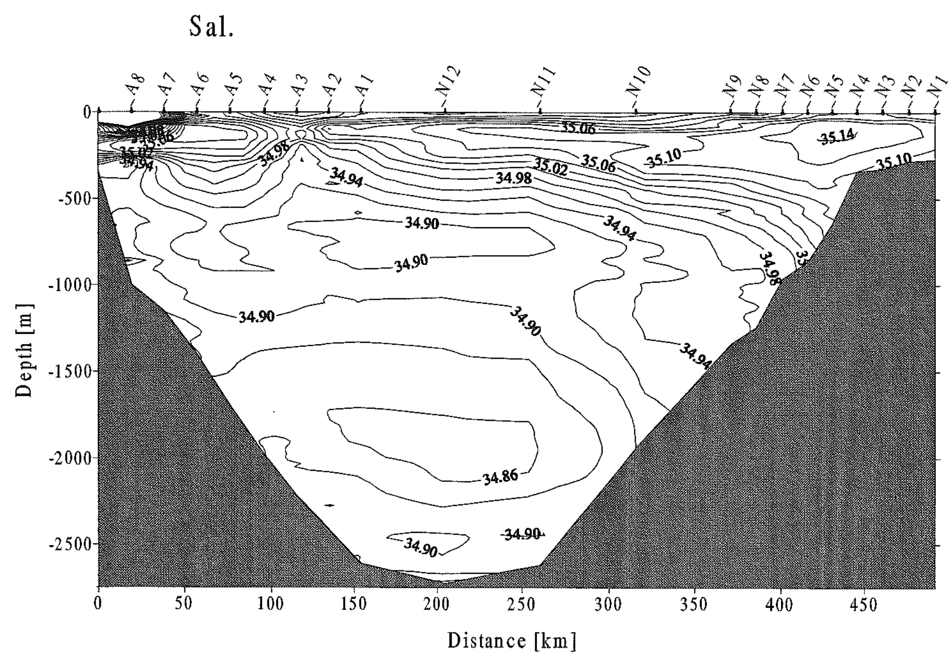
Sal.
A8
A7
A6
A5
A4
A3
A2
A1
N12
N11
N10
N9
N8
N7
N6
N5
N4
N3
N2
N1
35.06
35.14
35.02
35.06
35.10
35.10
34.98
34.94
34.98
34.90
34.94
34.90
34.98
34.90
34.90
34.94
34.86
34.90
34.90
0
-500
-1000
-1500
-2000
-2500
Depth [m]
0
50
100
150
200
250
300
350
400
450
Distance [km]

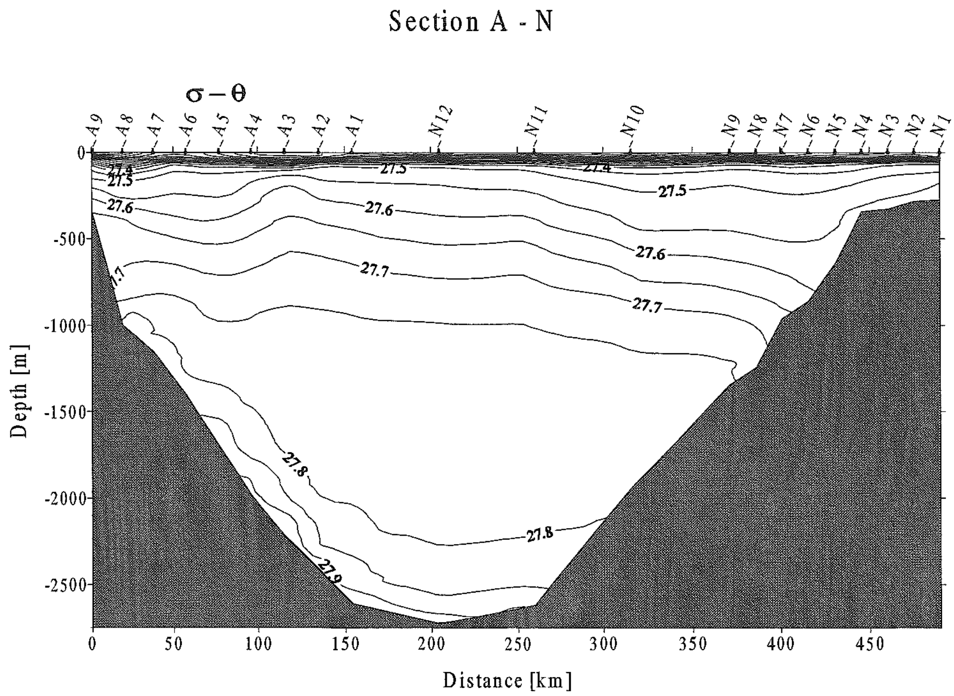
Section A - N
σ−θ
A9
A8
A7
A6
A5
A4
A3
A2
A1
N12
N11
N10
N9
N8
N7
N6
N5
N4
N3
N2
N1
27.5
27.4
27.6
27.7
27.8
27.9
Depth [m]
Distance [km]

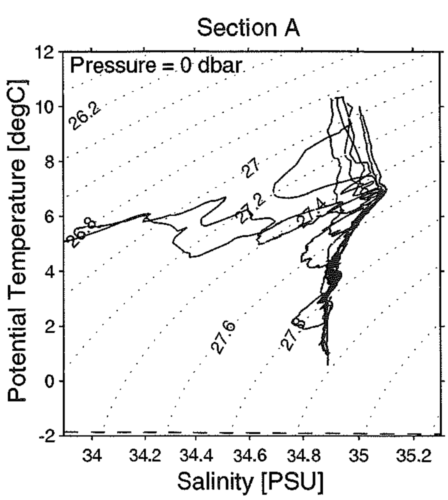
Section A
Pressure = 0 dbar
Potential Temperature [degC]
Salinity [PSU]
26.2
26.8
27
27.2
27.4
27.6
27.8

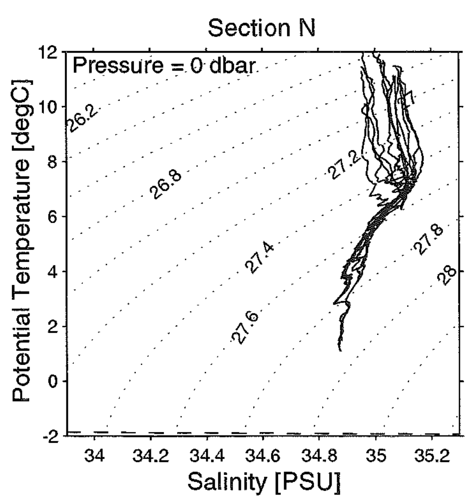
Section N
Pressure = 0 dbar
Potential Temperature [degC]
Salinity [PSU]
26.2
26.8
27
27.2
27.4
27.6
27.8
28

Section B

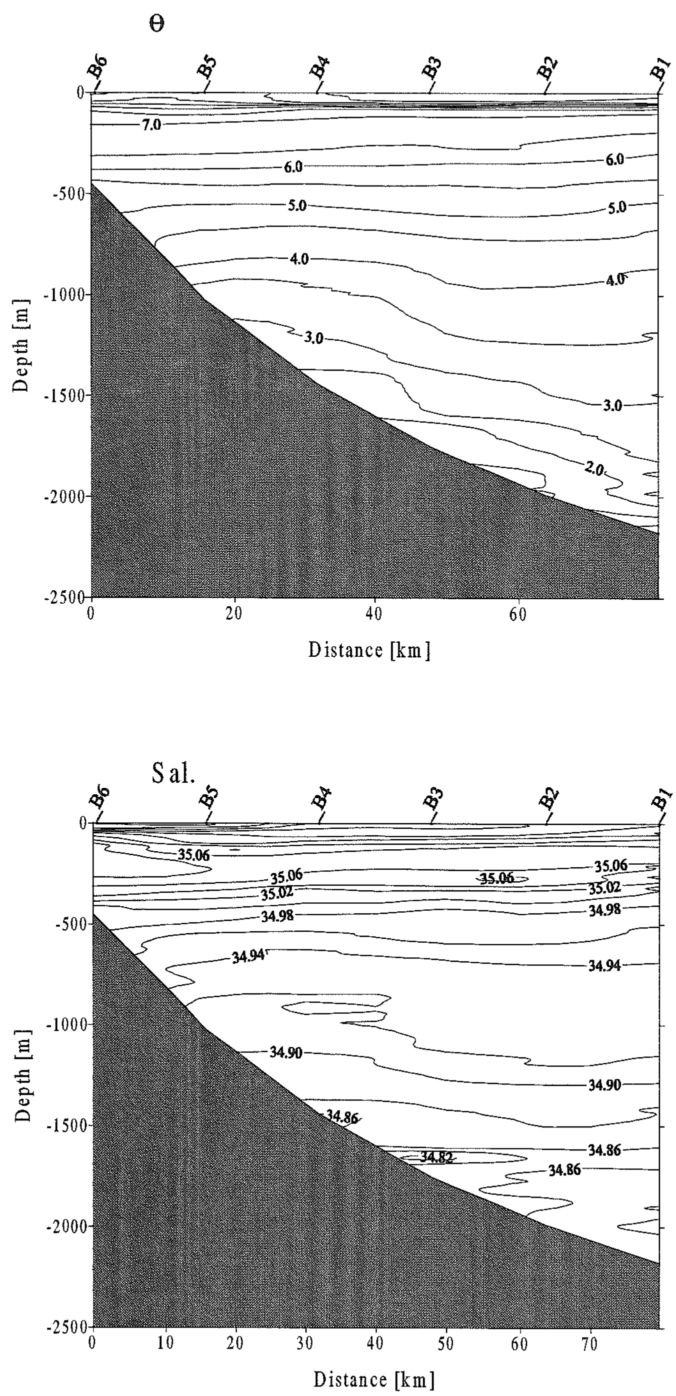
θ
B6
B5
B4
B3
B2
B1
7.0
6.0
5.0
4.0
3.0
2.0
Depth [m]
Distance [km]
Sal.
35.06
35.02
34.98
34.94
34.90
34.86
34.82

Section B

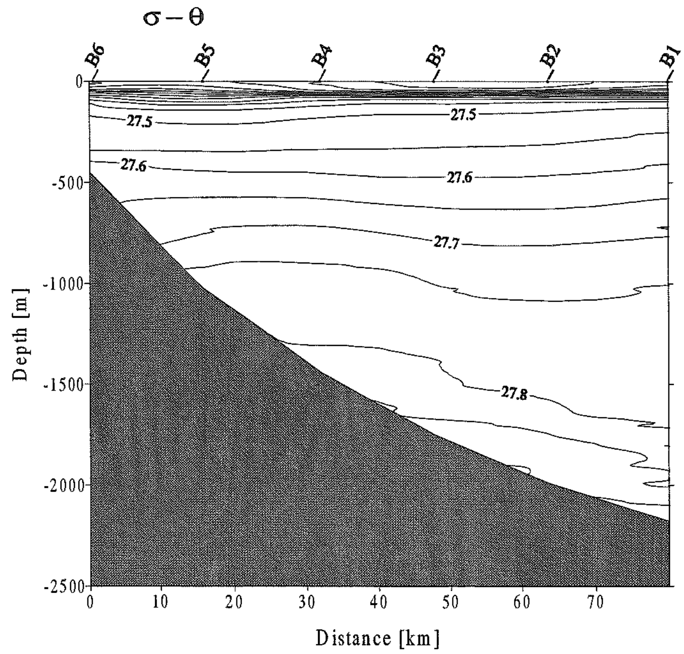
σ – θ
B6
B5
B4
B3
B2
B1
27.5
27.6
27.7
27.8
Depth [m]
Distance [km]

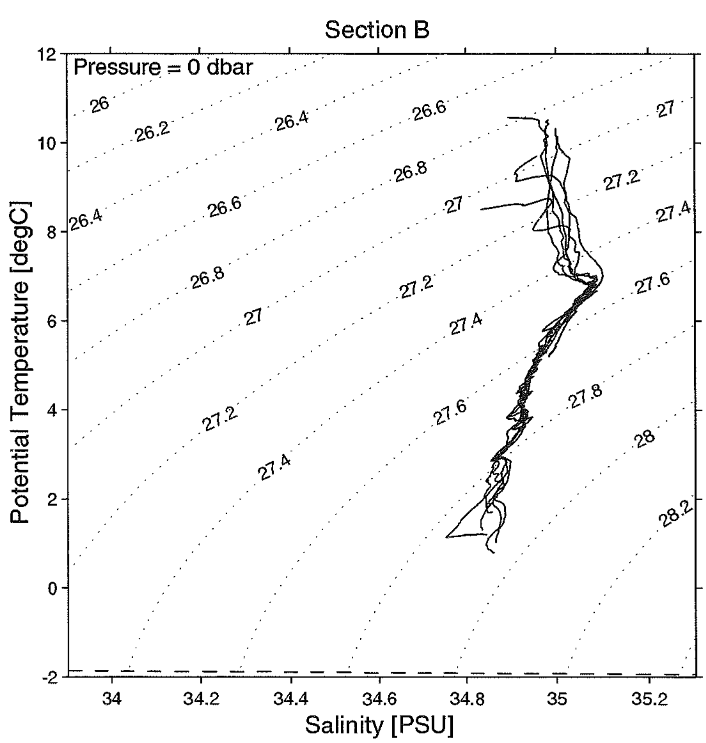
Section B
Pressure = 0 dbar
Potential Temperature [degC]
Salinity [PSU]

Section D

θ

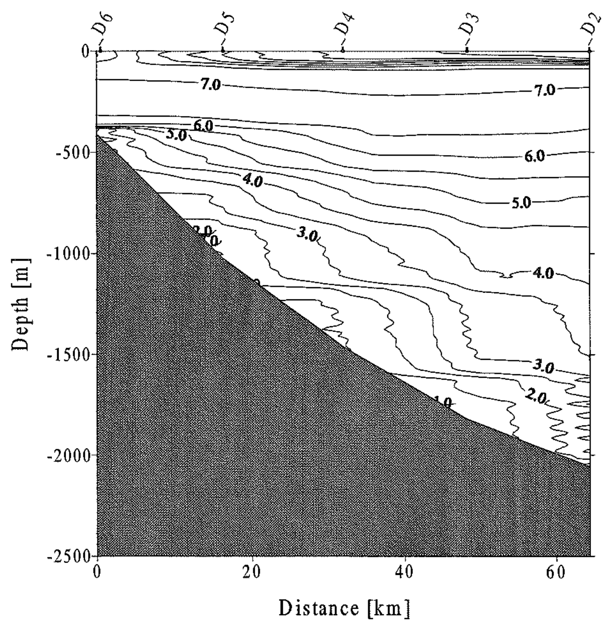

Sal.

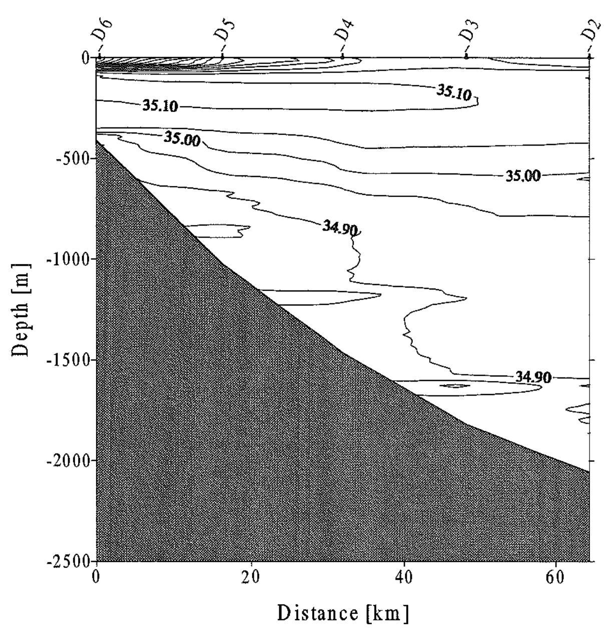

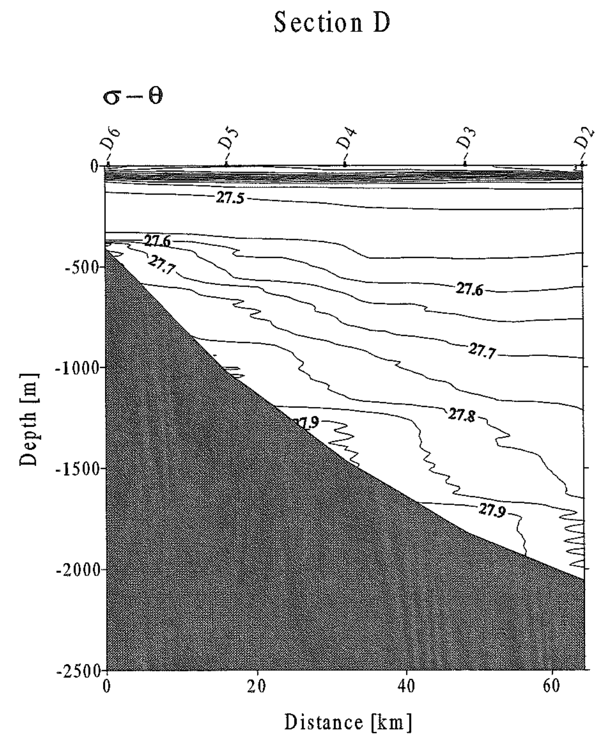
Section D
σ−θ
D6
D5
D4
D3
D2
27.5
27.6
27.7
27.6
27.7
27.8
27.9
27.9
Depth [m]
0
-500
-1000
-1500
-2000
-2500
0
20
40
60
Distance [km]

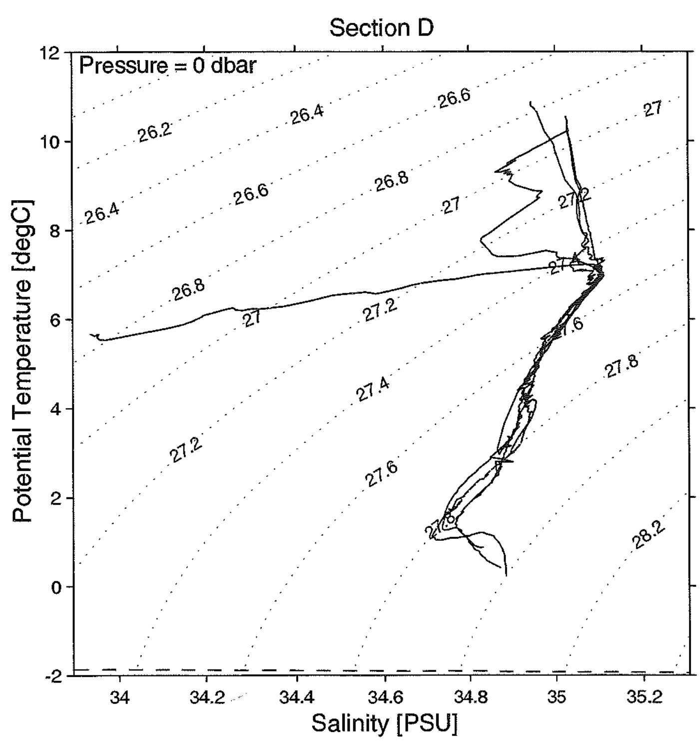
Section D
Pressure = 0 dbar
26.2
26.4
26.6
27
26.4
26.6
26.8
27
26.8
27
27.2
27.4
27.6
27.8
27.2
27.6
28.2
Potential Temperature [degC]
12
10
8
6
4
2
0
-2
34
34.2
34.4
34.6
34.8
35
35.2
Salinity [PSU]

Section E, crossing 1

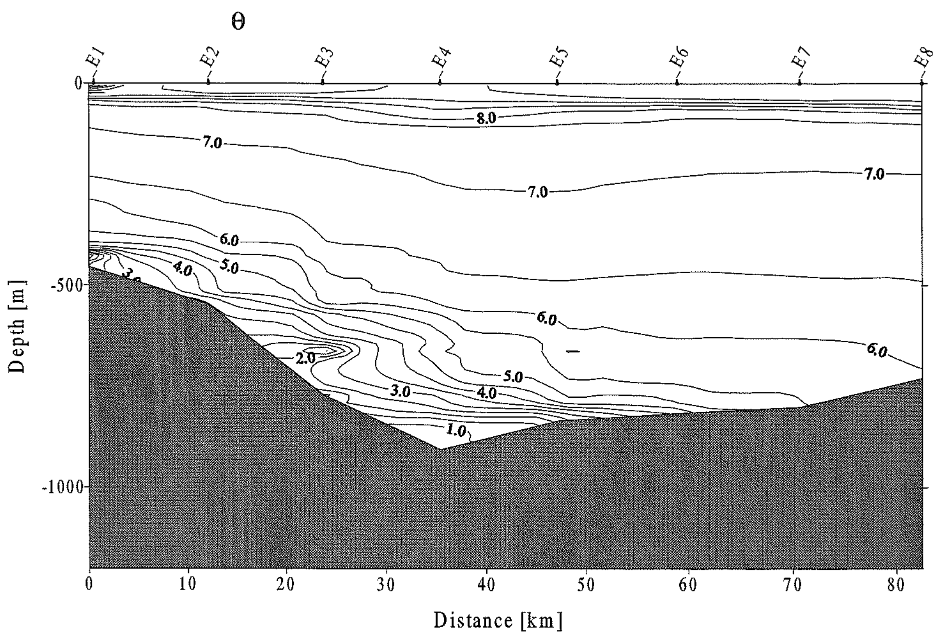

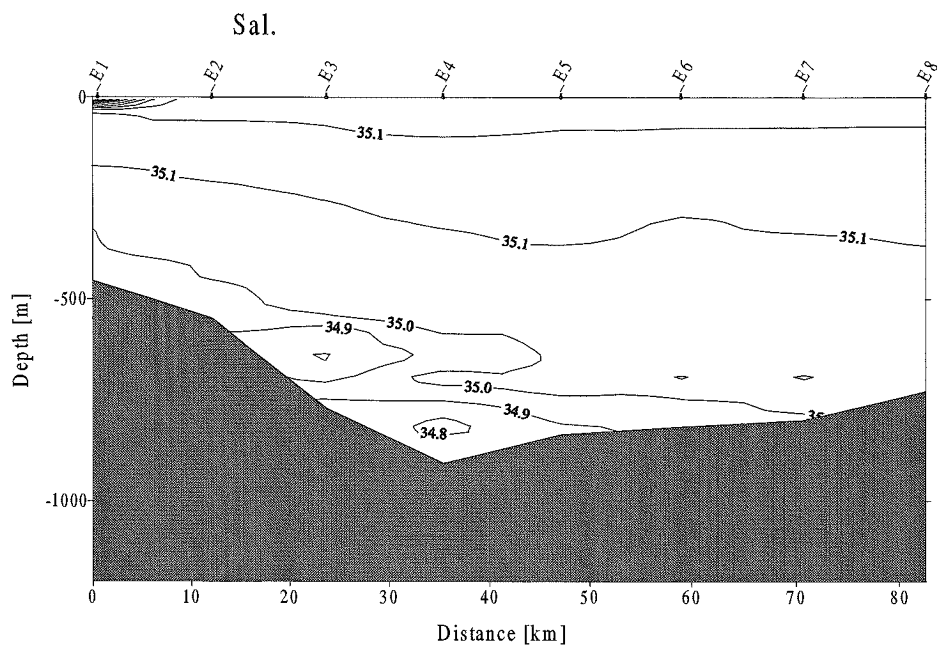

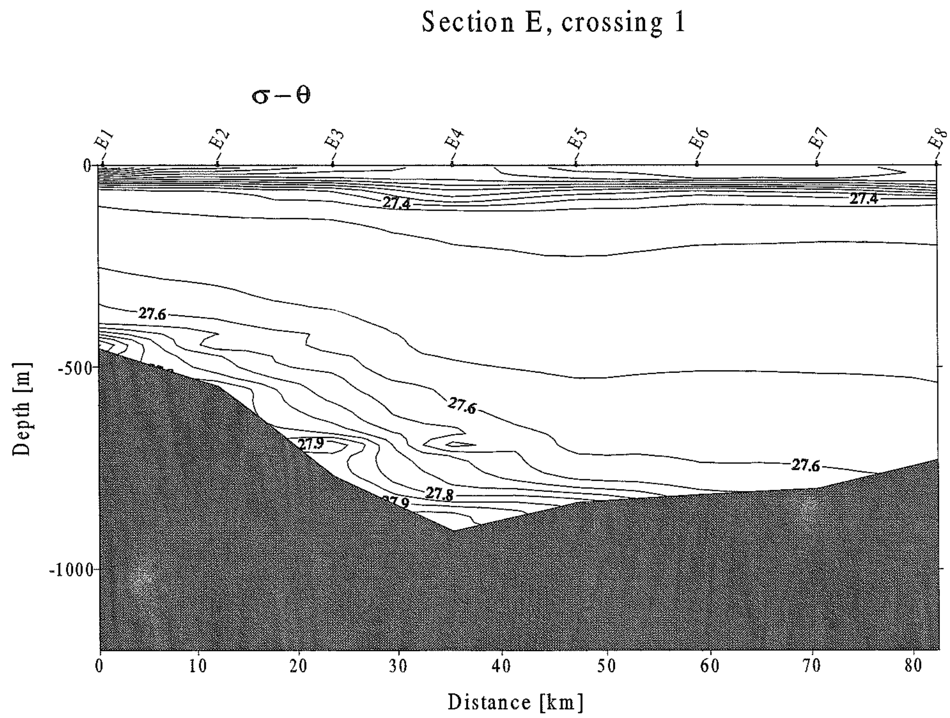
Section E, crossing 1
σ−θ
E1
E2
E3
E4
E5
E6
E7
E8
27.4
27.4
27.6
27.6
27.6
27.9
27.8
27.9
Depth [m]
0
-500
-1000
Distance [km]
0
10
20
30
40
50
60
70
80

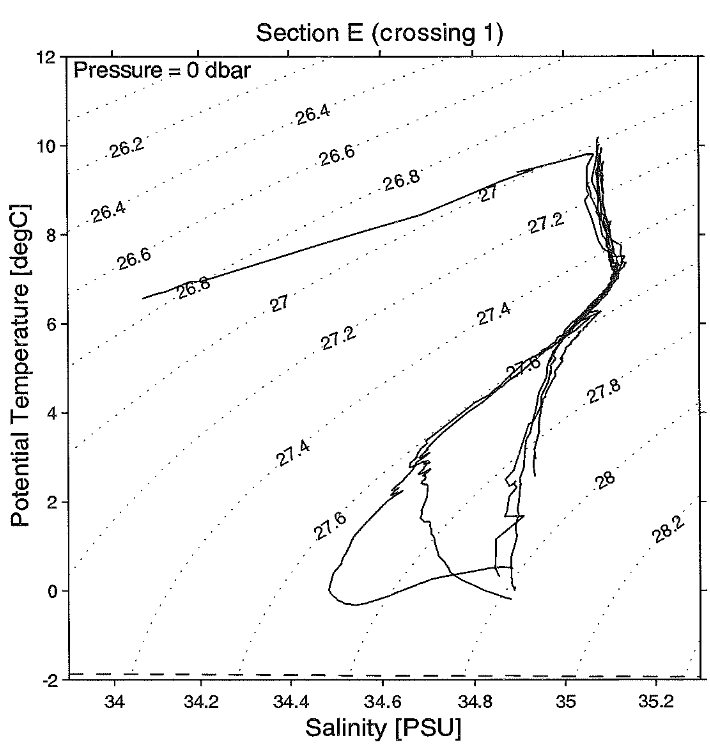
Section E (crossing 1)
Pressure = 0 dbar
Potential Temperature [degC]
Salinity [PSU]
12
10
8
6
4
2
0
-2
34
34.2
34.4
34.6
34.8
35
35.2
26.2
26.4
26.6
26.8
27
27.2
27.4
27.6
27.8
28
28.2

Section E, crossing 2

θ

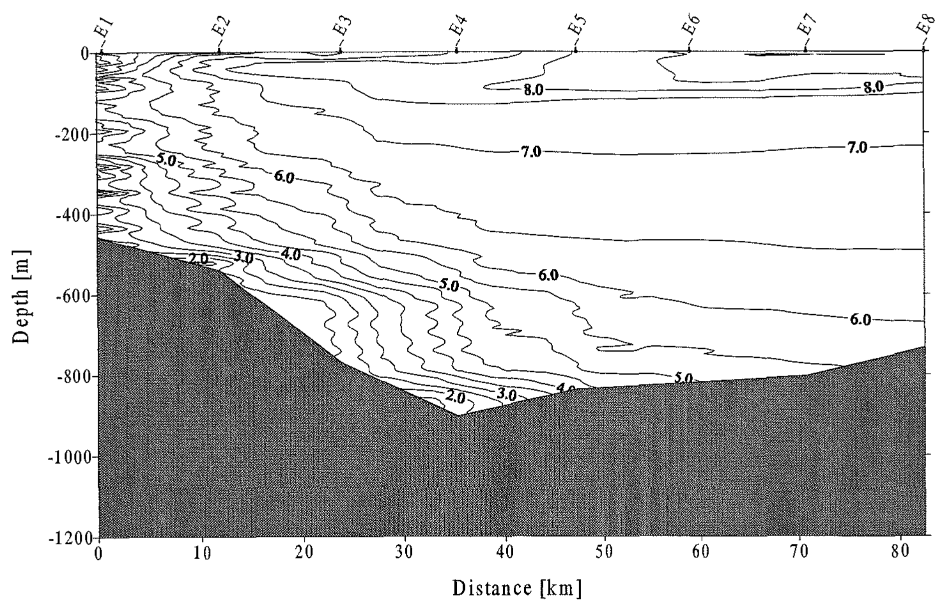

Sal.

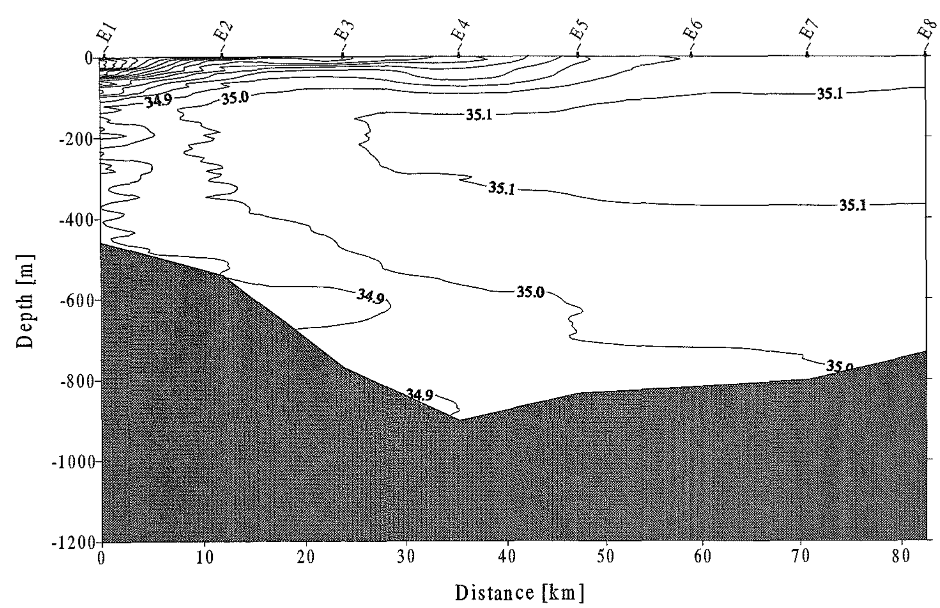

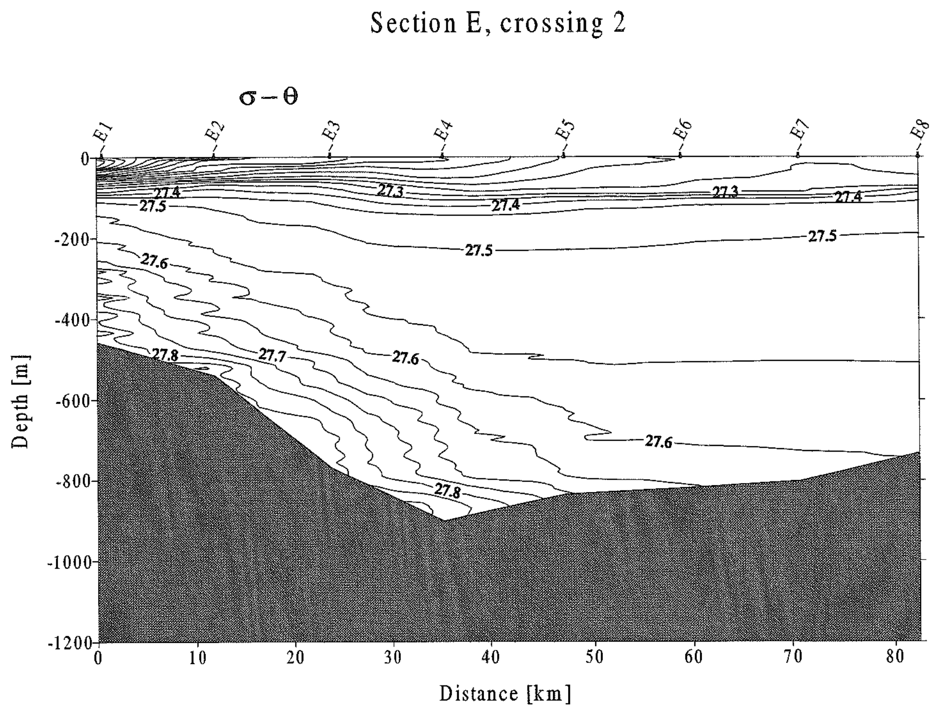

Section E, crossing 2
σ−θ
E1
E2
E3
E4
E5
E6
E7
E8
27.3
27.4
27.5
27.6
27.7
27.8
Depth [m]
Distance [km]

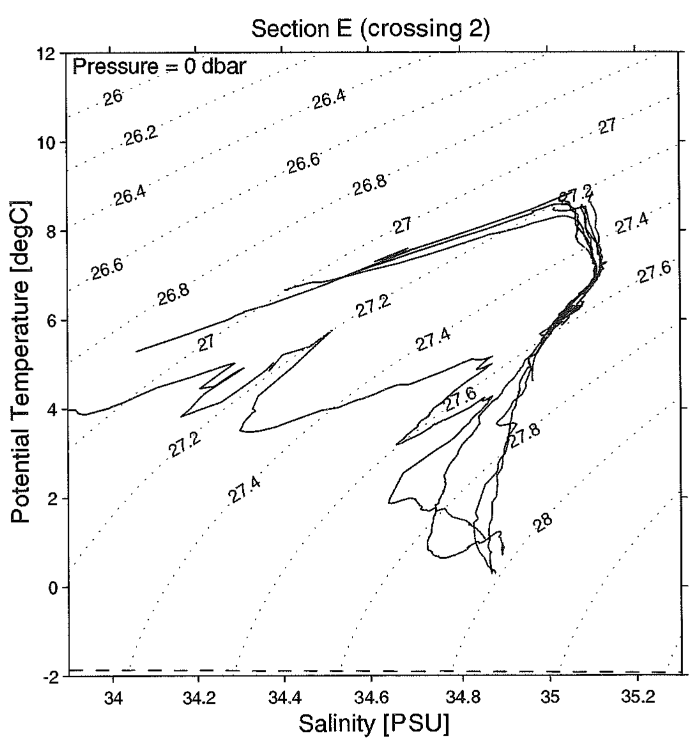

Section E (crossing 2)
Pressure = 0 dbar
Potential Temperature [degC]
Salinity [PSU]

Section H

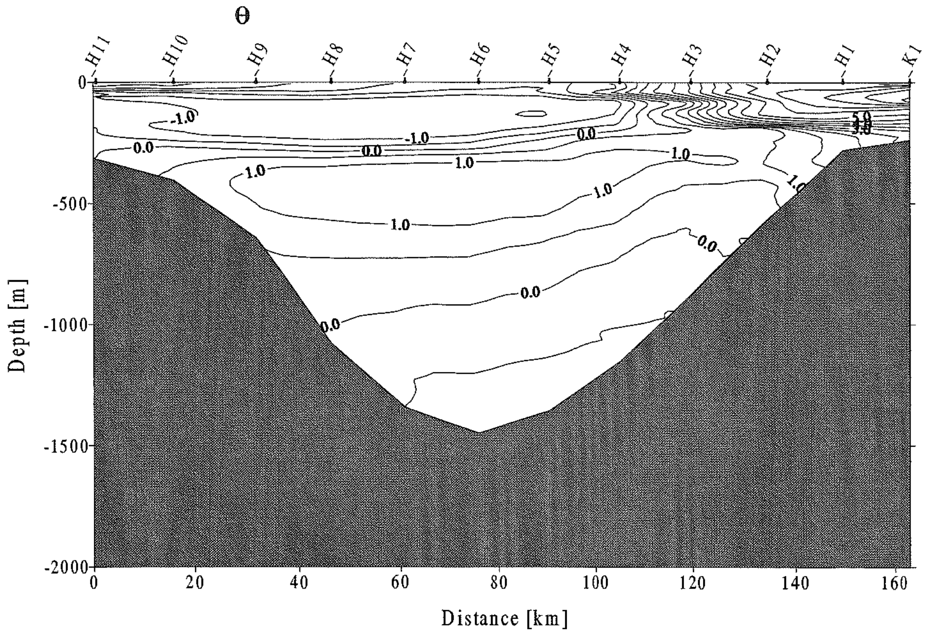
Θ
H11
H10
H9
H8
H7
H6
H5
H4
H3
H2
H1
K1
-1.0
0.0
1.0
5.0
3.0
Depth [m]
0
-500
-1000
-1500
-2000
0
20
40
60
80
100
120
140
160
Distance [km]

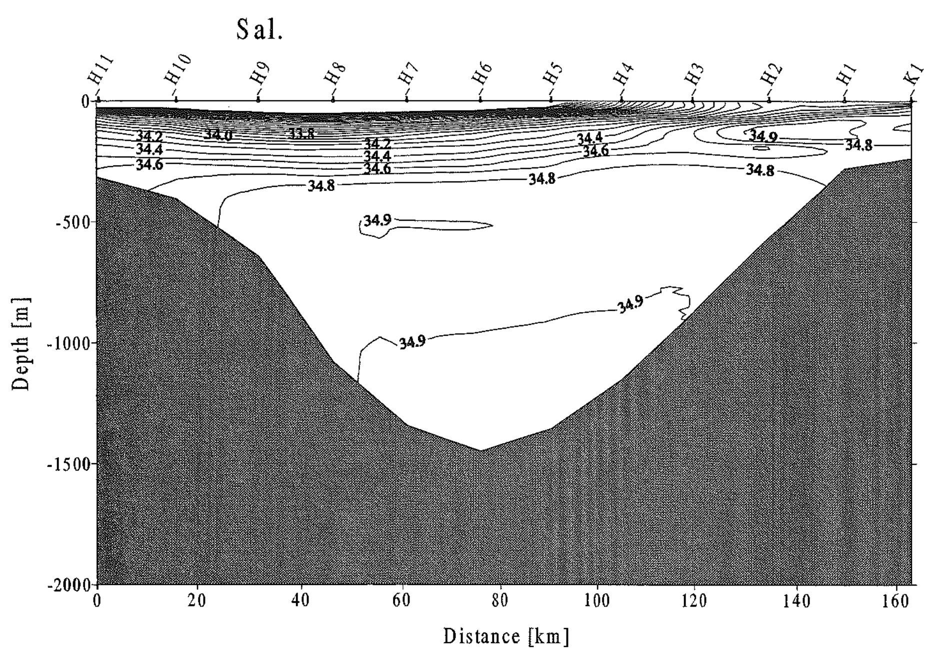
Sal.
H11
H10
H9
H8
H7
H6
H5
H4
H3
H2
H1
K1
34.2
34.4
34.6
34.0
33.8
34.8
34.9
Depth [m]
0
-500
-1000
-1500
-2000
0
20
40
60
80
100
120
140
160
Distance [km]

Section H

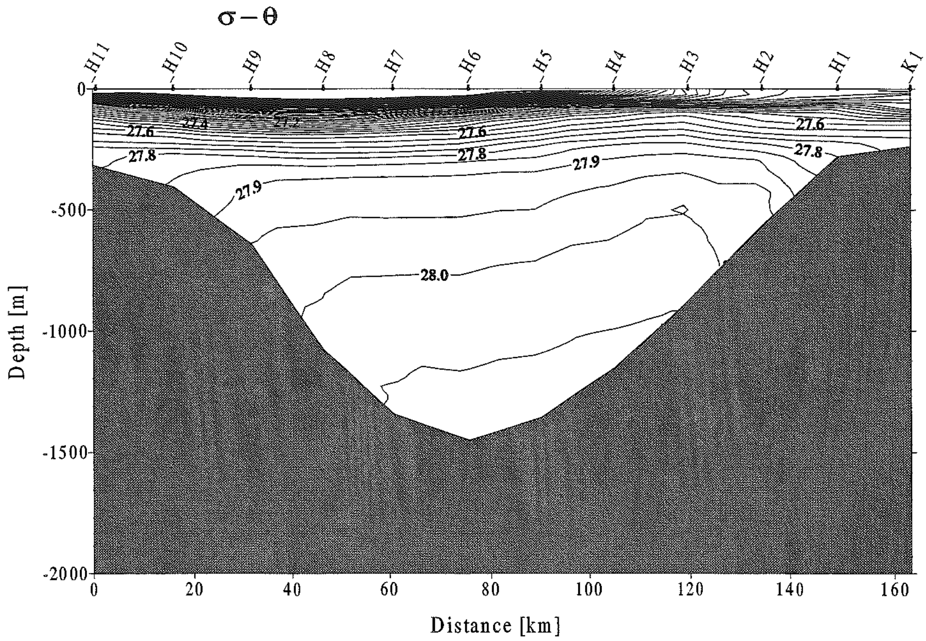
σ−θ
H11
H10
H9
H8
H7
H6
H5
H4
H3
H2
H1
K1
27.6
27.4
27.8
27.6
27.8
27.9
27.6
27.8
27.9
28.0
0
-500
-1000
-1500
-2000
Depth [m]
0
20
40
60
80
100
120
140
160
Distance [km]

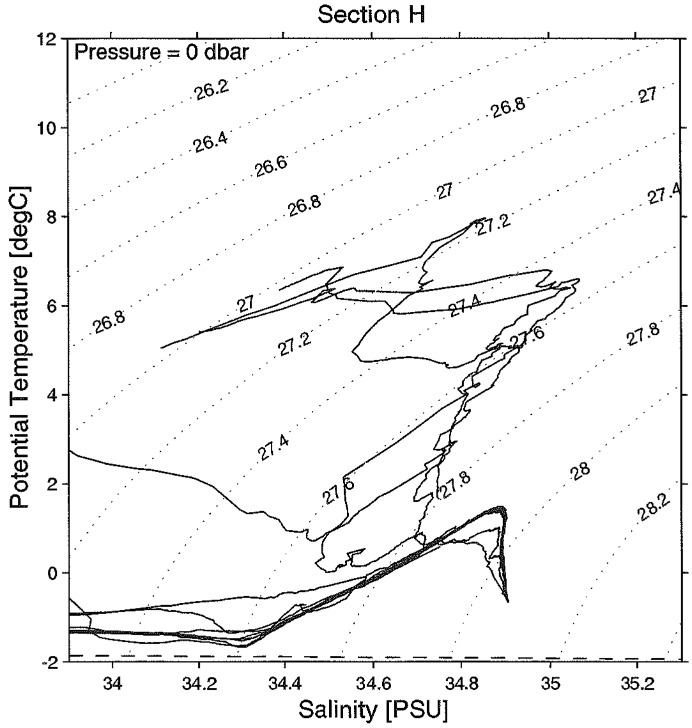
Section H
Pressure = 0 dbar
Potential Temperature [degC]
Salinity [PSU]
12
10
8
6
4
2
0
-2
34
34.2
34.4
34.6
34.8
35
35.2

Section J

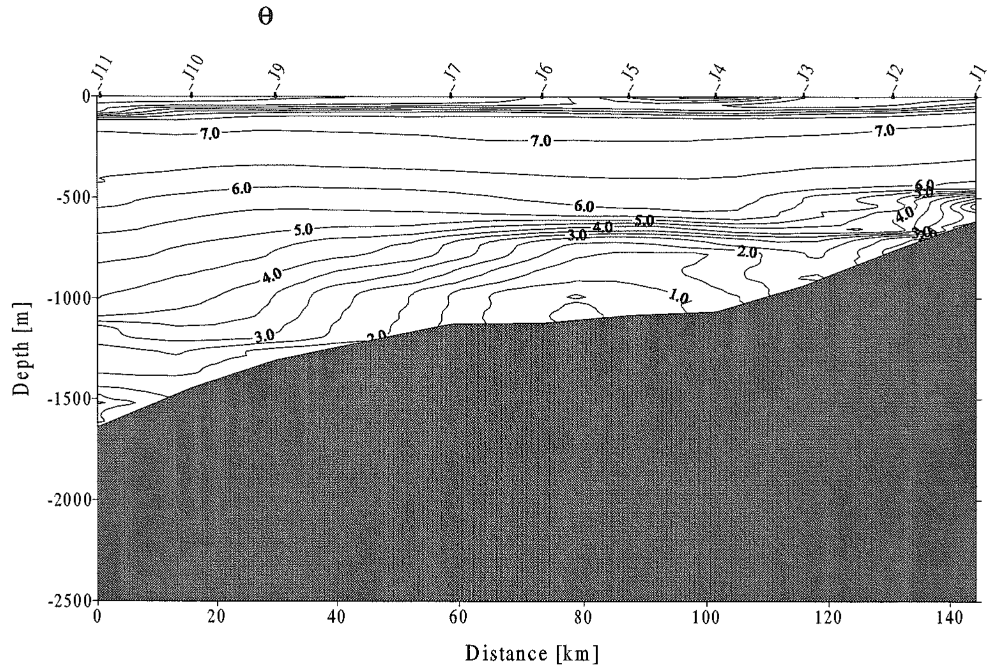
θ
J11
J10
J9
J7
J6
J5
J4
J3
J2
J1
7.0
6.0
5.0
4.0
3.0
2.0
1.0
0
-500
-1000
-1500
-2000
-2500
Depth [m]
0
20
40
60
80
100
120
140
Distance [km]

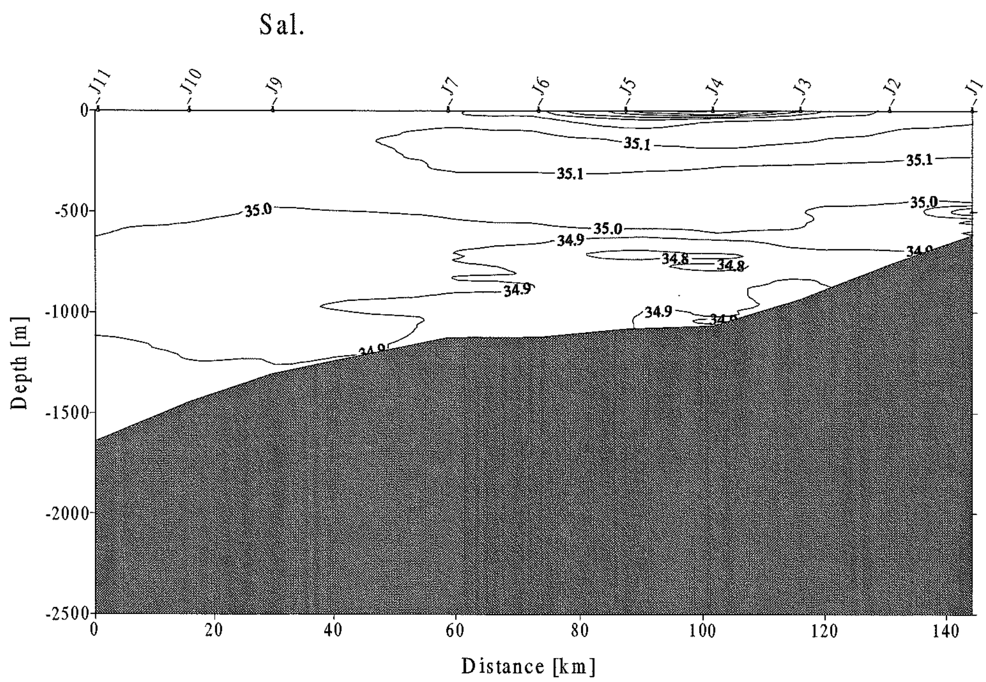
Sal.
J11
J10
J9
J7
J6
J5
J4
J3
J2
J1
35.1
35.0
34.9
34.8
0
-500
-1000
-1500
-2000
-2500
Depth [m]
0
20
40
60
80
100
120
140
Distance [km]

Section J

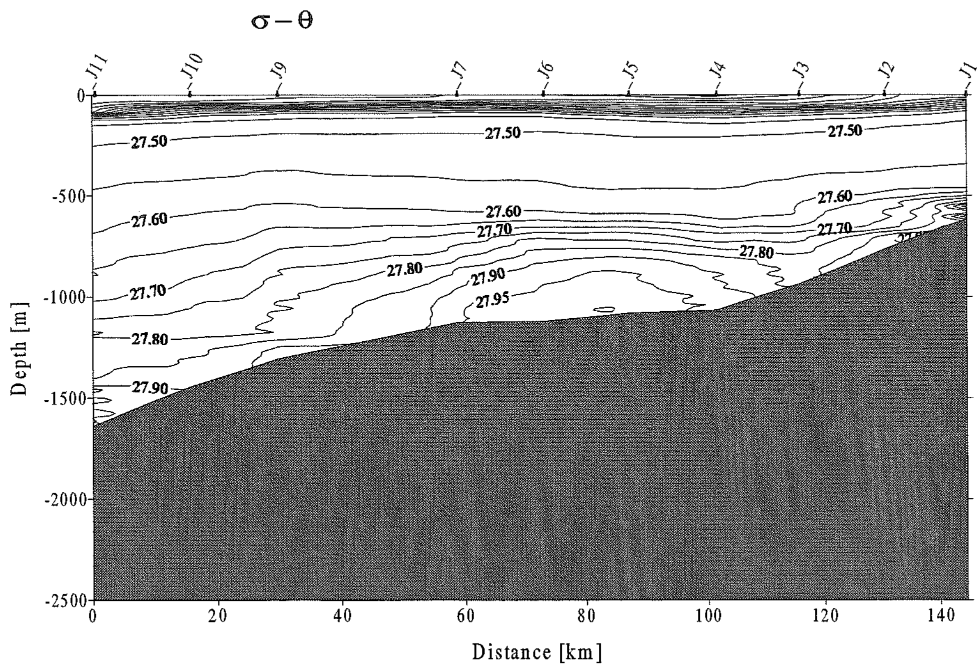
σ−θ
J11
J10
J9
J7
J6
J5
J4
J3
J2
J1
27.50
27.60
27.70
27.80
27.90
27.95
Depth [m]
Distance [km]

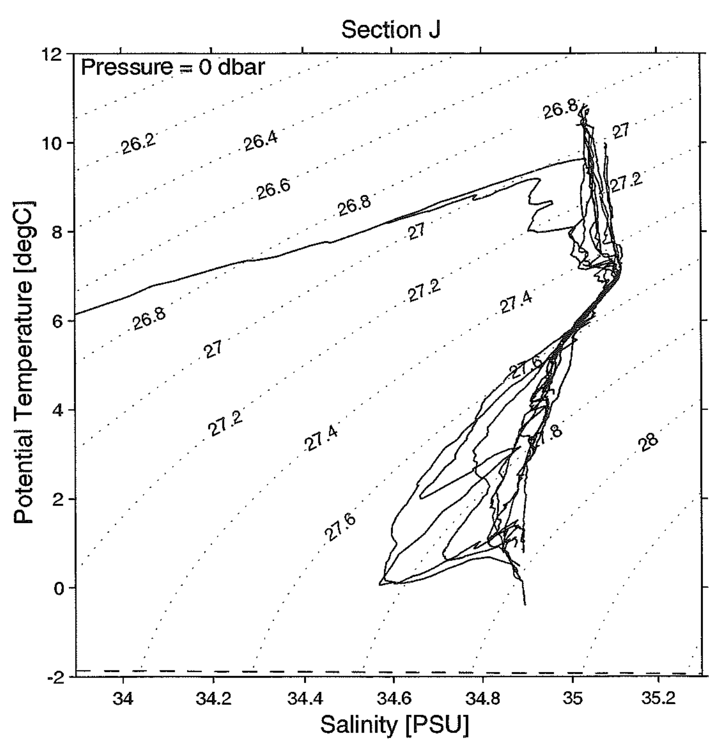
Section J
Pressure = 0 dbar
26.2
26.4
26.6
26.8
27
27.2
27.4
27.6
27.8
28
Potential Temperature [degC]
Salinity [PSU]

Section K

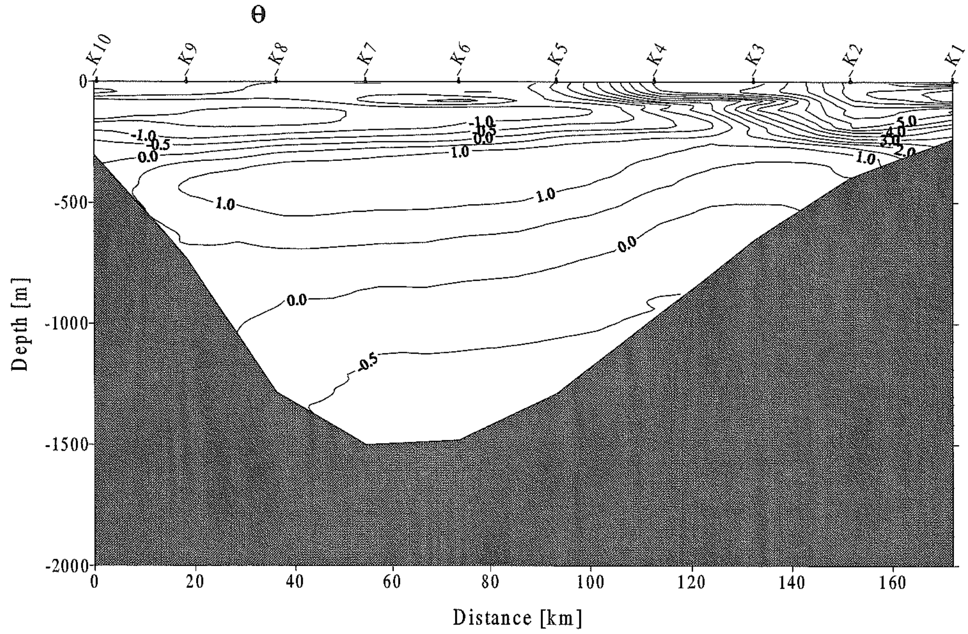
θ
K10
K9
K8
K7
K6
K5
K4
K3
K2
K1
Depth [m]
0
-500
-1000
-1500
-2000
Distance [km]
0
20
40
60
80
100
120
140
160
1.0
0.0
-.0.5

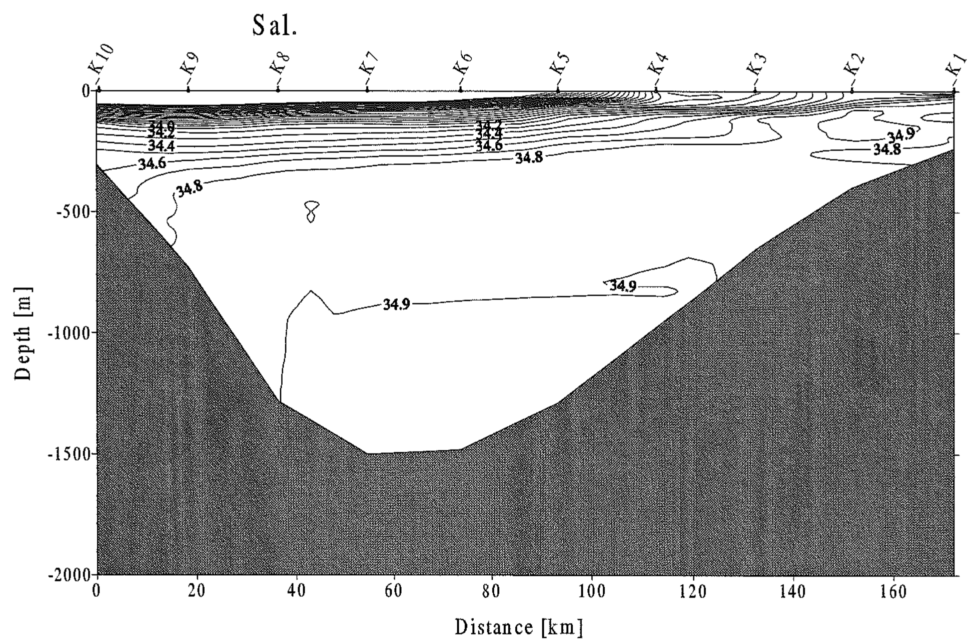
Sal.
K10
K9
K8
K7
K6
K5
K4
K3
K2
K1
Depth [m]
0
-500
-1000
-1500
-2000
Distance [km]
0
20
40
60
80
100
120
140
160
34.6
34.8
34.9

Section K

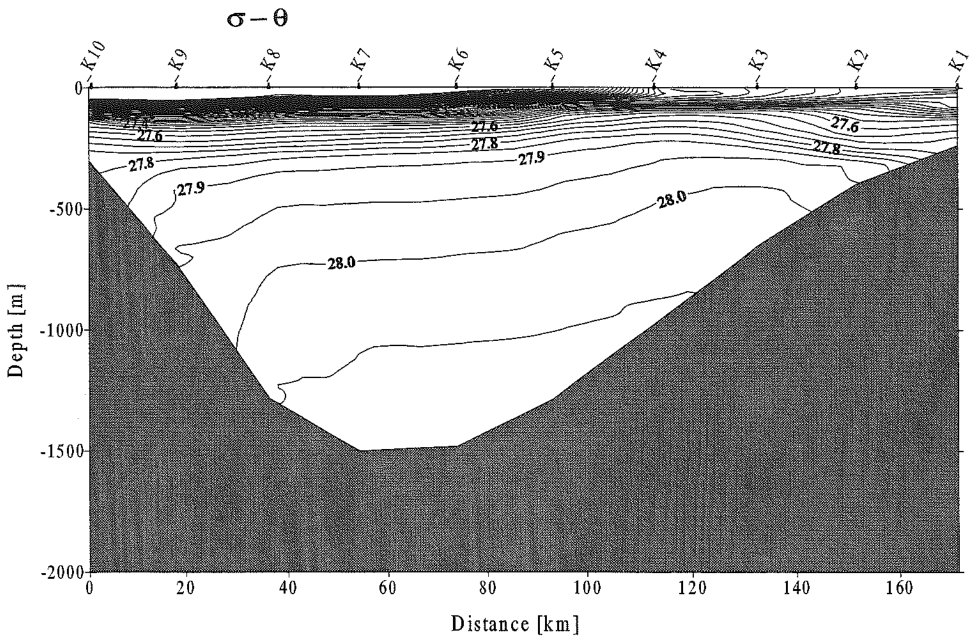
σ−θ
K10
K9
K8
K7
K6
K5
K4
K3
K2
K1
27.6
27.8
27.9
28.0
Depth [m]
0
-500
-1000
-1500
-2000
0
20
40
60
80
100
120
140
160
Distance [km]

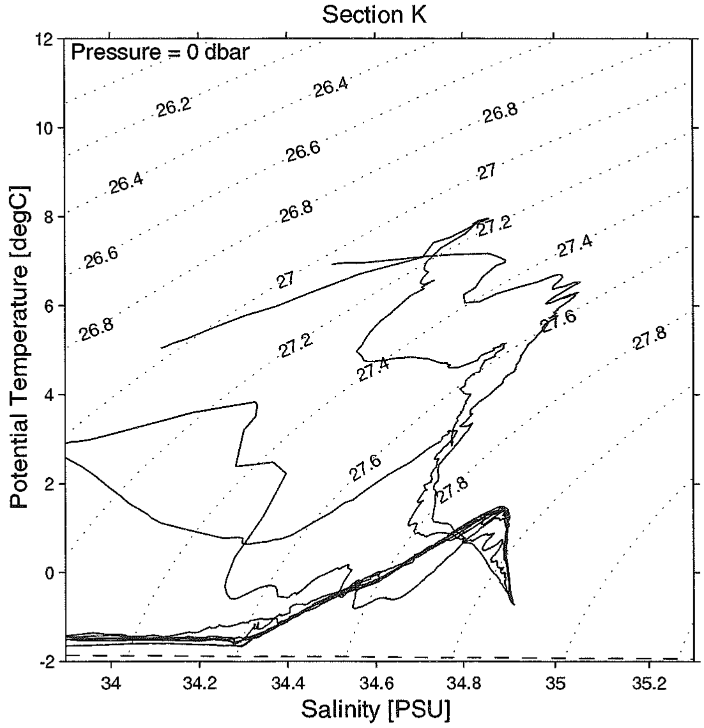
Section K
Pressure = 0 dbar
Potential Temperature [degC]
Salinity [PSU]
12
10
8
6
4
2
0
-2
34
34.2
34.4
34.6
34.8
35
35.2
26.2
26.4
26.6
26.8
27
27.2
27.4
27.6
27.8

Section L, crossing 1

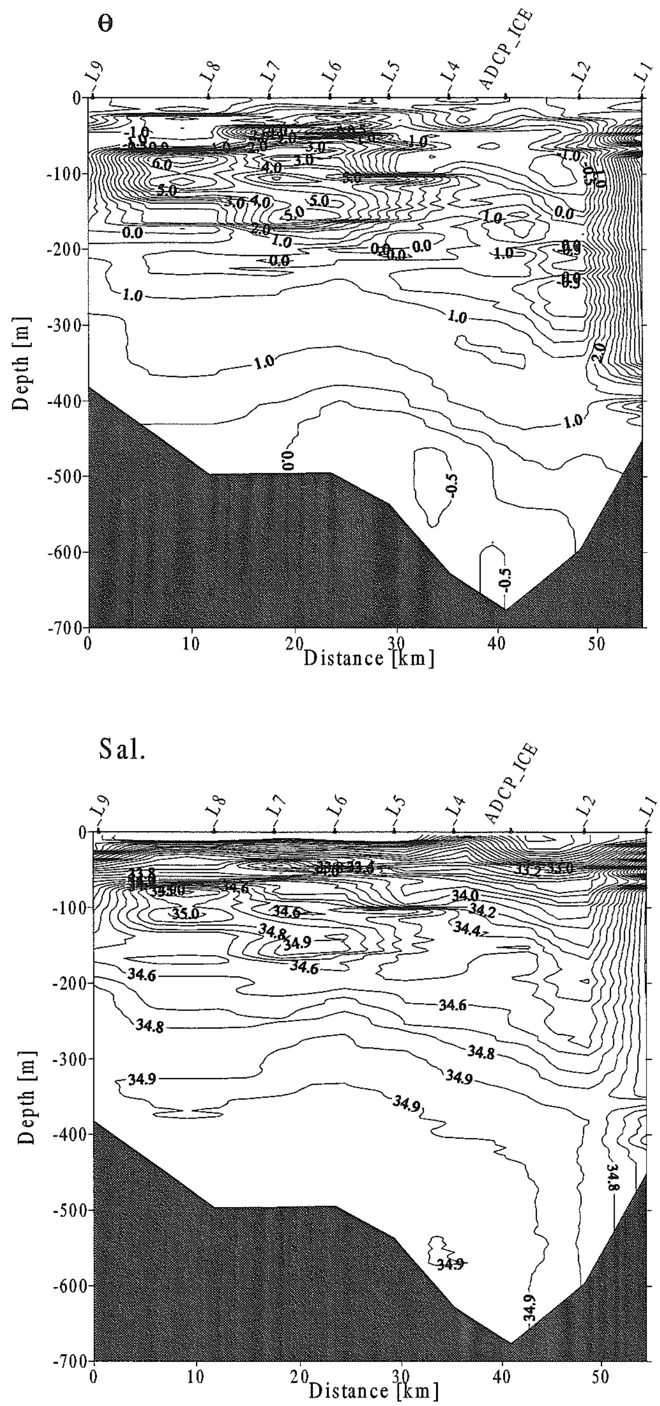

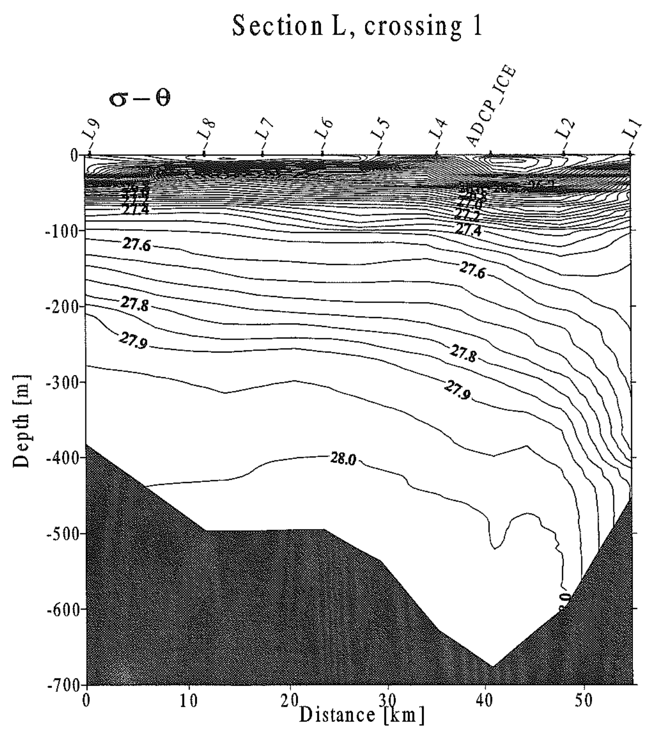
Section L, crossing 1
σ−θ
L9
L8
L7
L6
L5
L4
ADCP_ICE
L2
L1
27.6
27.8
27.9
28.0
Depth [m]
Distance [km]

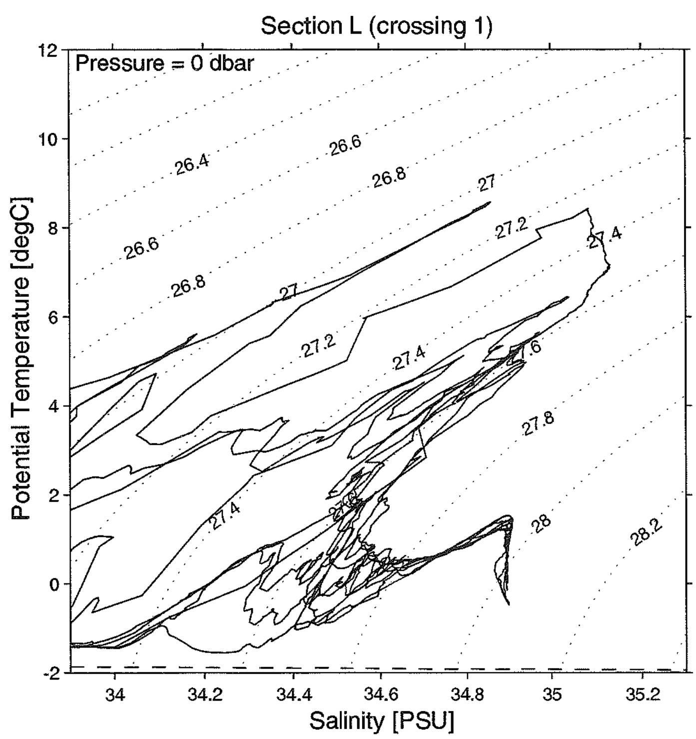
Section L (crossing 1)
Pressure = 0 dbar
Potential Temperature [degC]
Salinity [PSU]

Section L, crossing 2

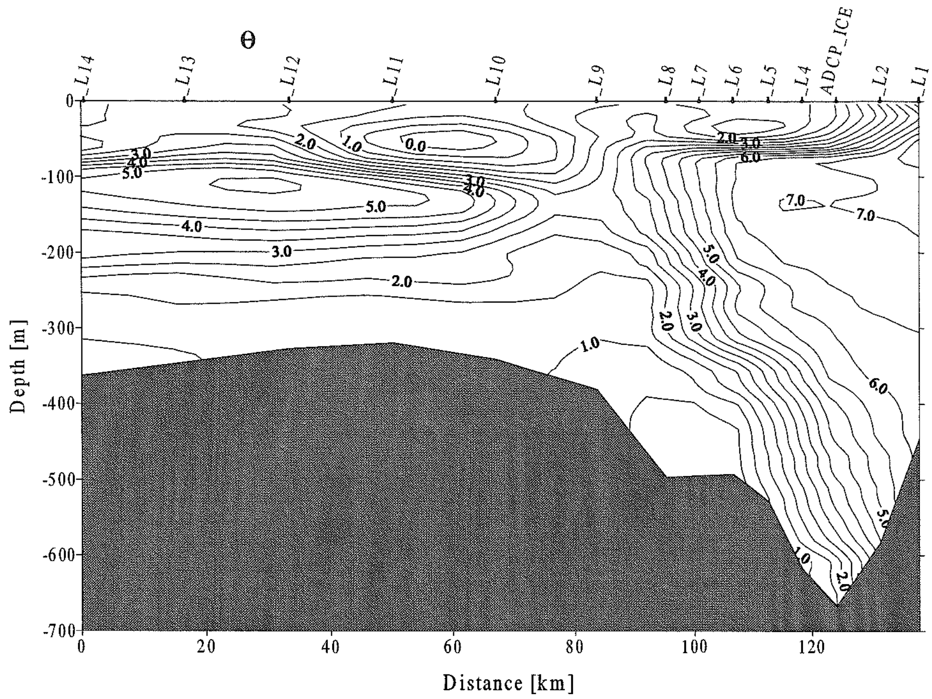

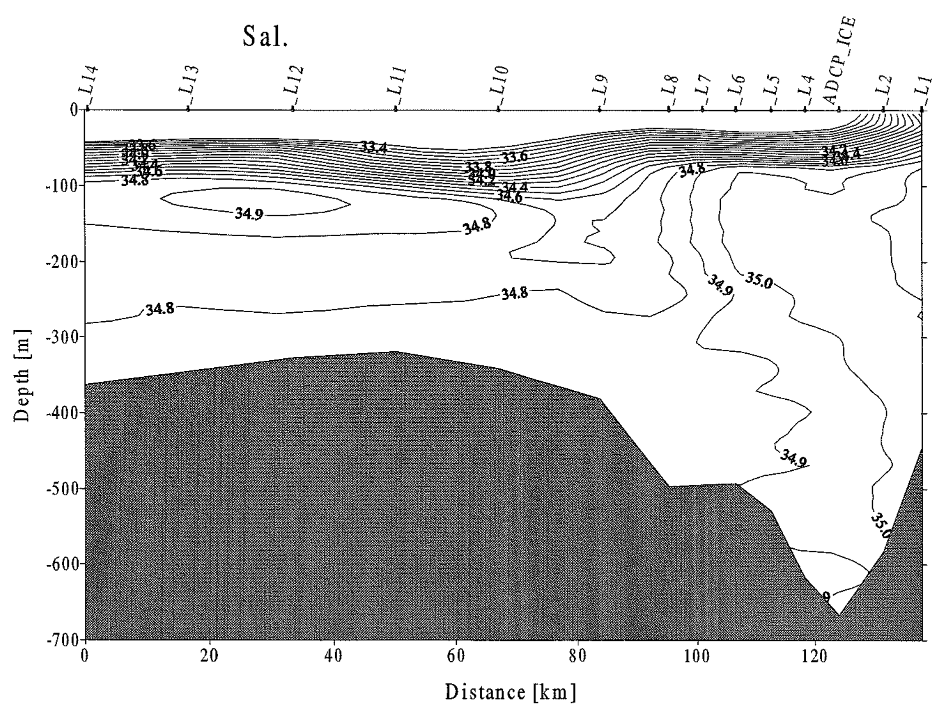

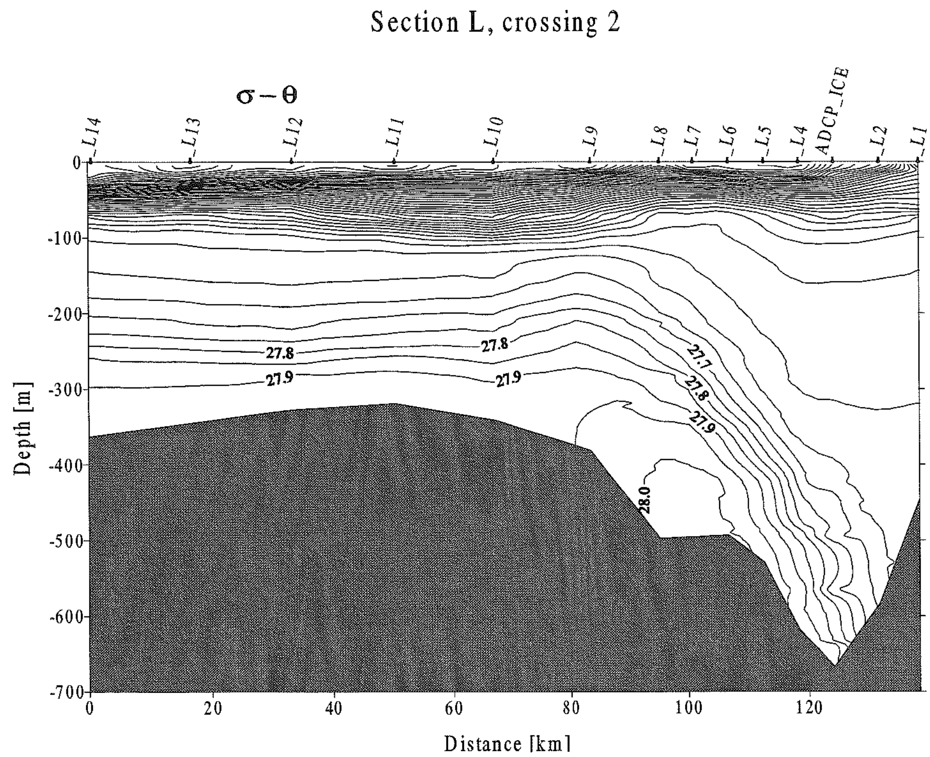
Section L, crossing 2
σ−θ
L14
L13
L12
L11
L10
L9
L8
L7
L6
L5
L4
ADCP_ICE
L2
L1
27.8
27.9
27.7
28.0
Depth [m]
Distance [km]

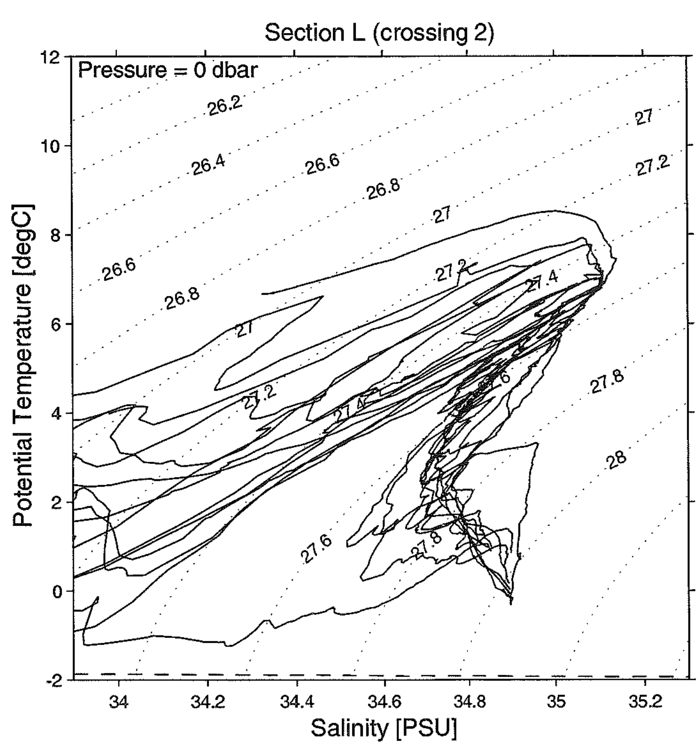
Section L (crossing 2)
Pressure = 0 dbar
Potential Temperature [degC]
Salinity [PSU]

Section L, crossing 3

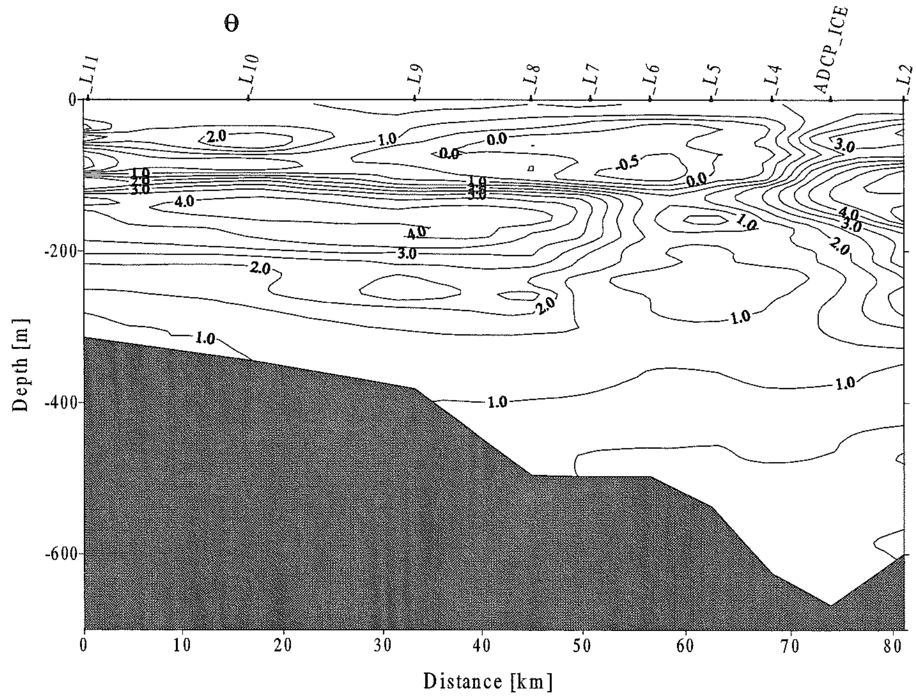

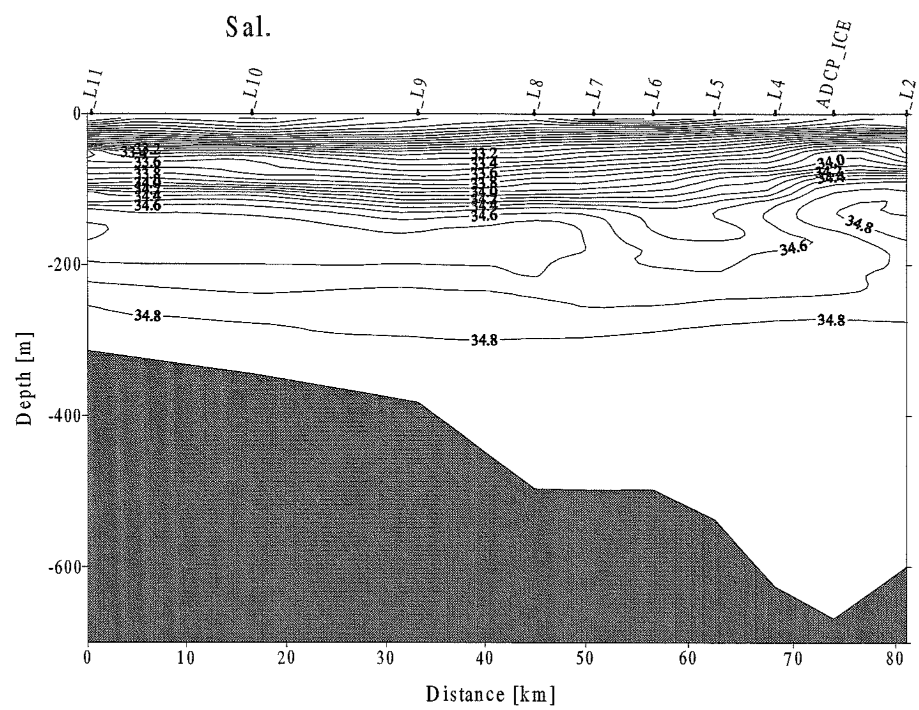

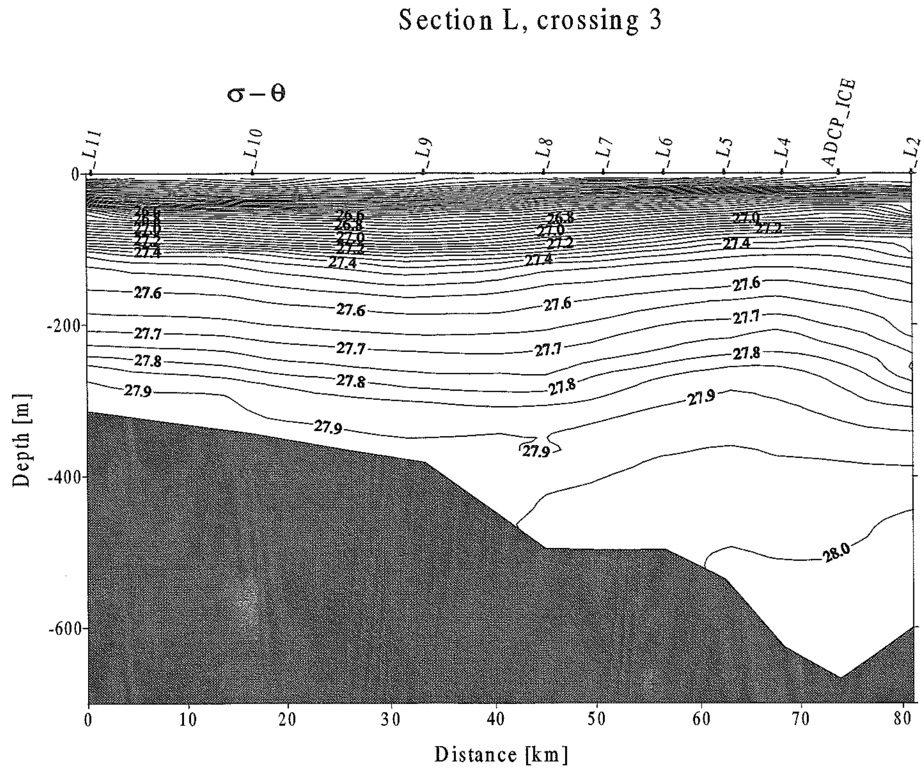
Section L, crossing 3
σ-θ
L11
L10
L9
L8
L7
L6
L5
L4
ADCP_ICE
L2
Depth [m]
Distance [km]
27.6
27.7
27.8
27.9
28.0

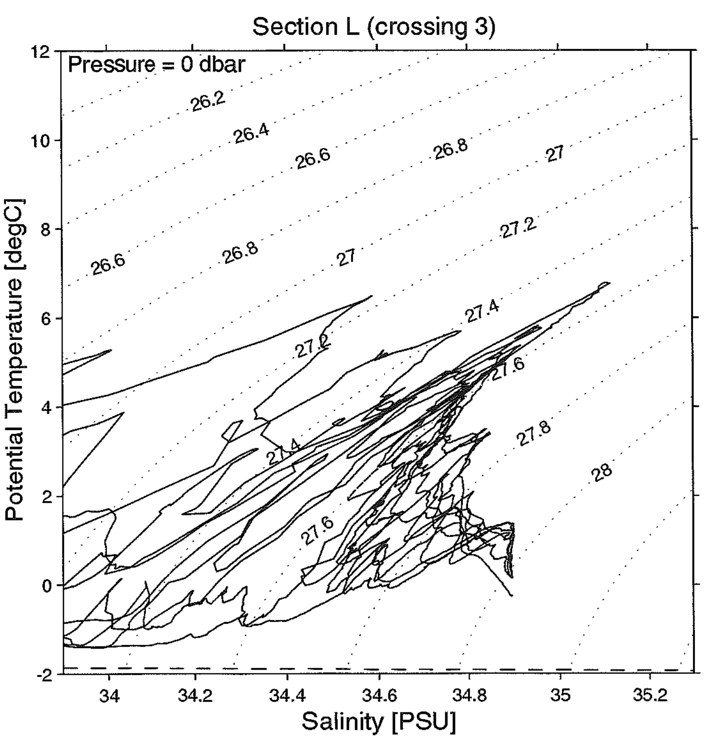
Section L (crossing 3)
Pressure = 0 dbar
Potential Temperature [degC]
Salinity [PSU]

Section M (Cross section SW-NE)

θ

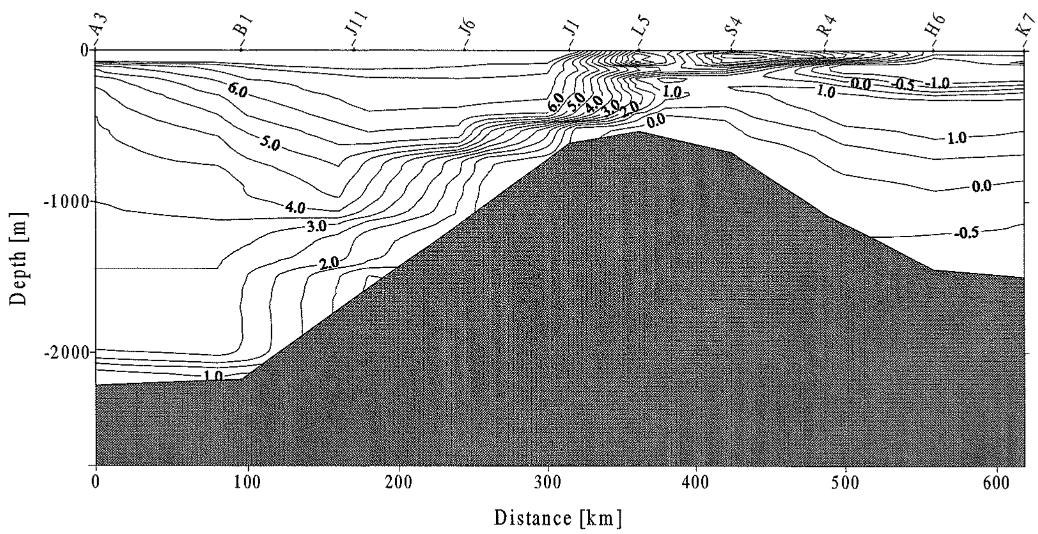

Sal.

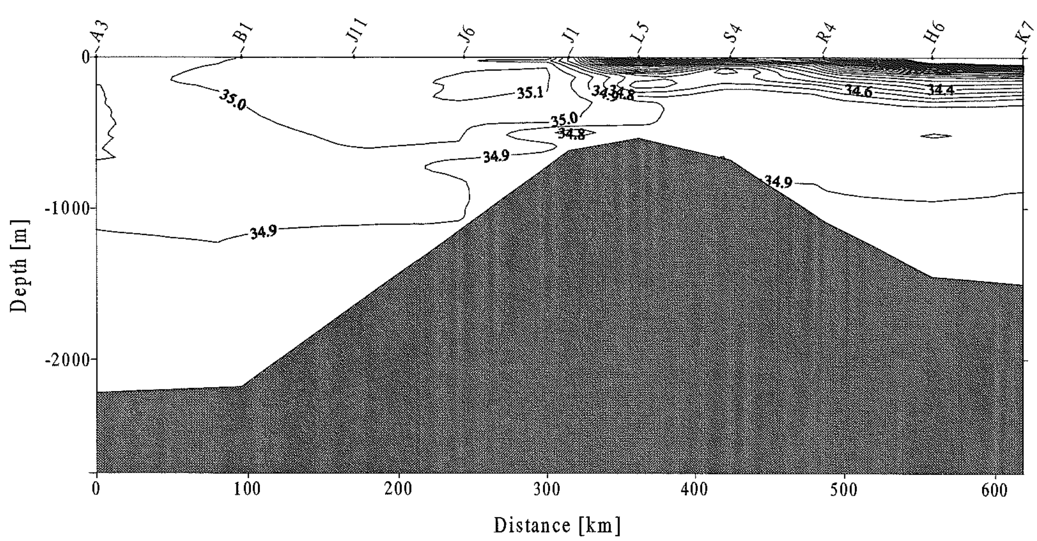

Section M (Cross section SW-NE)

σ−θ

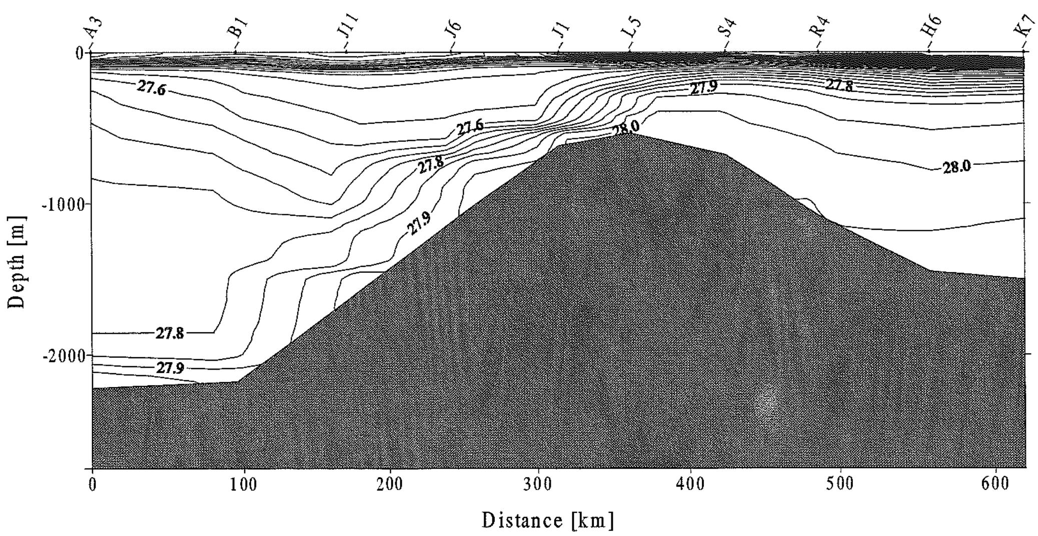

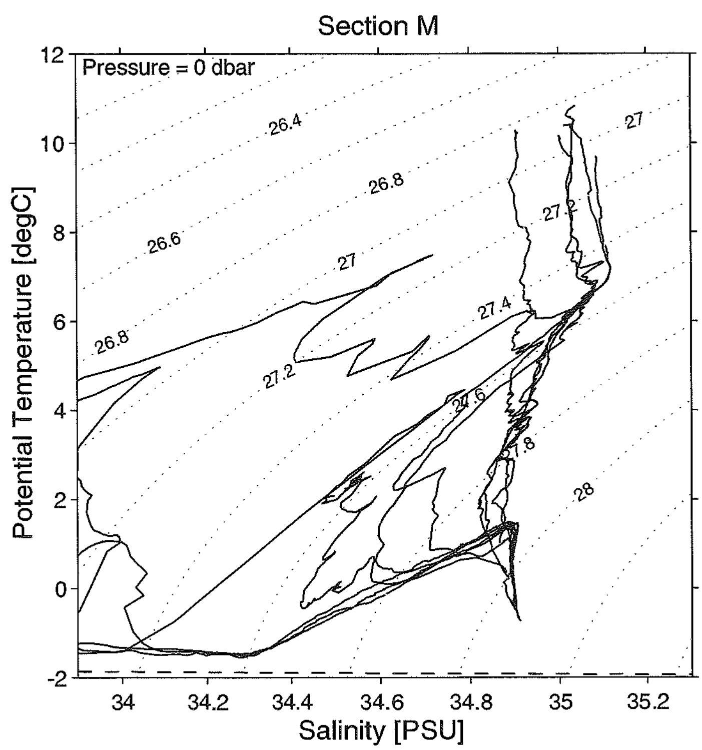

Section R

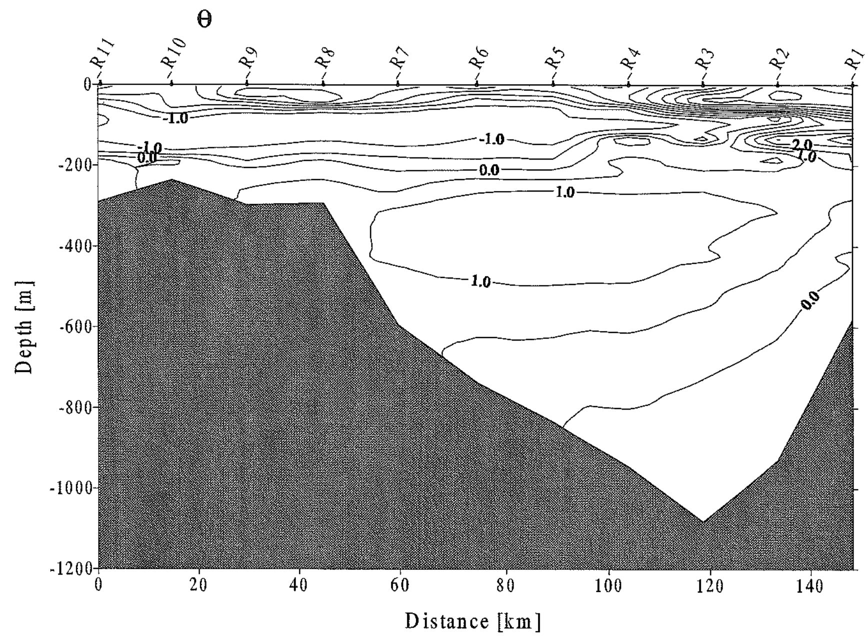
θ
R11
R10
R9
R8
R7
R6
R5
R4
R3
R2
R1
-1.0
-1.0
0.0
-1.0
0.0
1.0
1.0
0.0
2.0
1.0
Depth [m]
0
-200
-400
-600
-800
-1000
-1200
0
20
40
60
80
100
120
140
Distance [km]

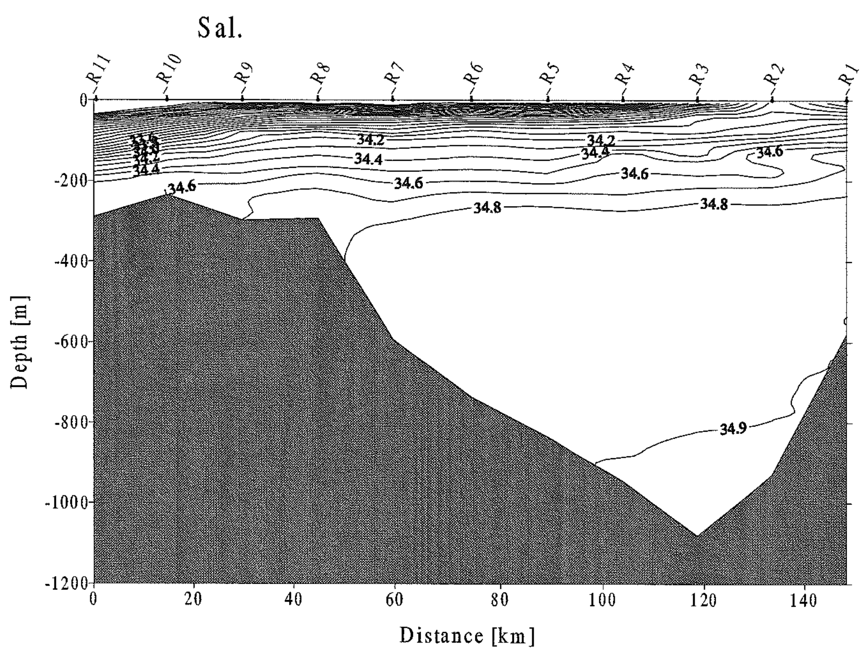
Sal.
R11
R10
R9
R8
R7
R6
R5
R4
R3
R2
R1
34.2
34.4
34.2
34.4
34.6
34.6
34.6
34.6
34.8
34.8
34.9
Depth [m]
0
-200
-400
-600
-800
-1000
-1200
0
20
40
60
80
100
120
140
Distance [km]

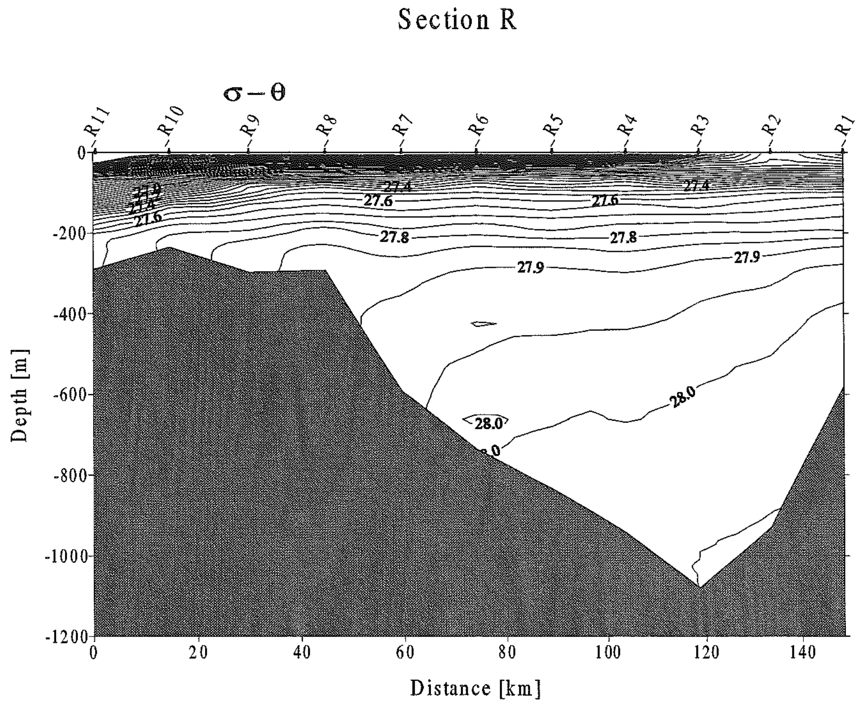
Section R
σ−θ
R11
R10
R9
R8
R7
R6
R5
R4
R3
R2
R1
27.4
27.6
27.8
27.9
28.0
Depth [m]
Distance [km]

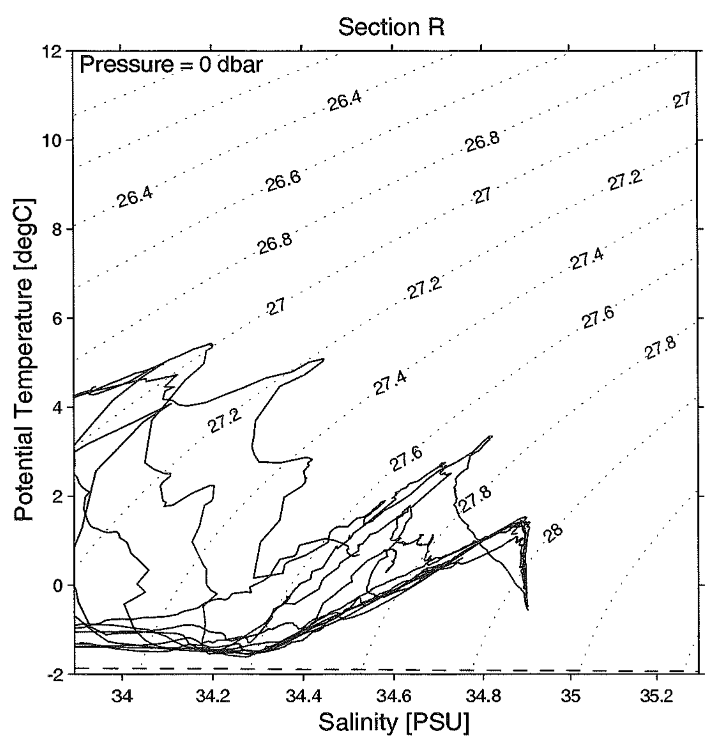
Section R
Pressure = 0 dbar
Potential Temperature [degC]
Salinity [PSU]

Section S, crossing 1

θ

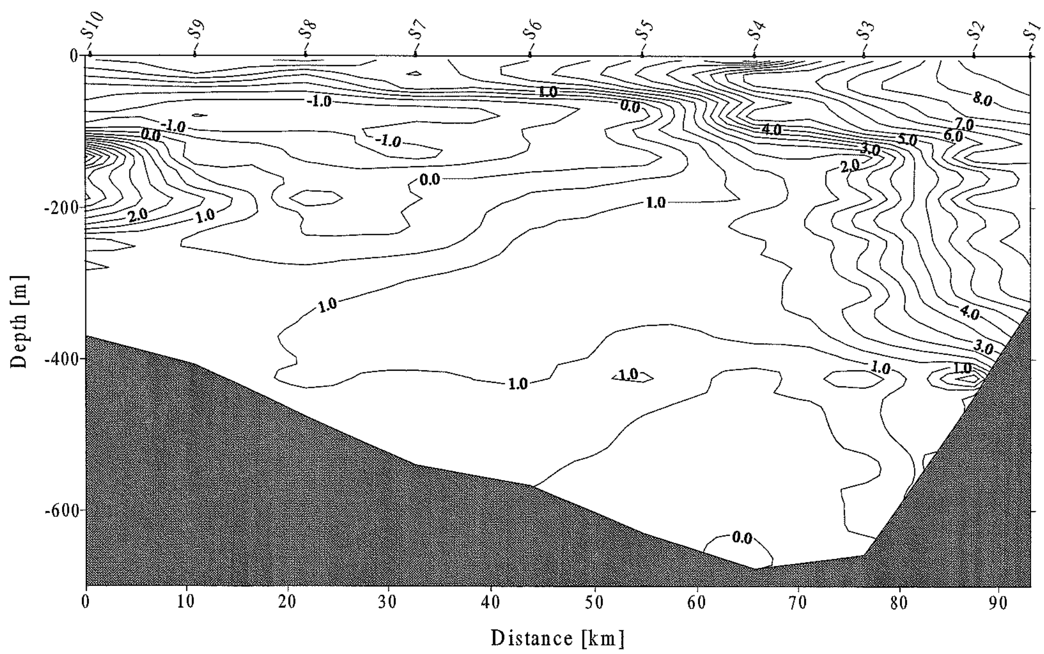

Sal.

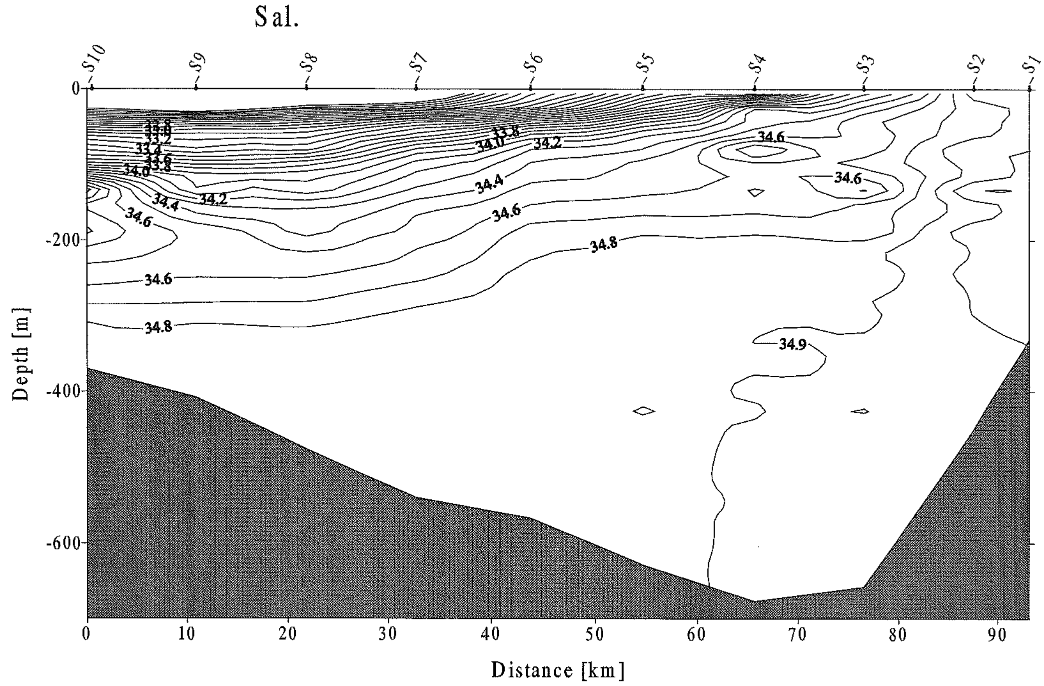

Section S, crossing 1

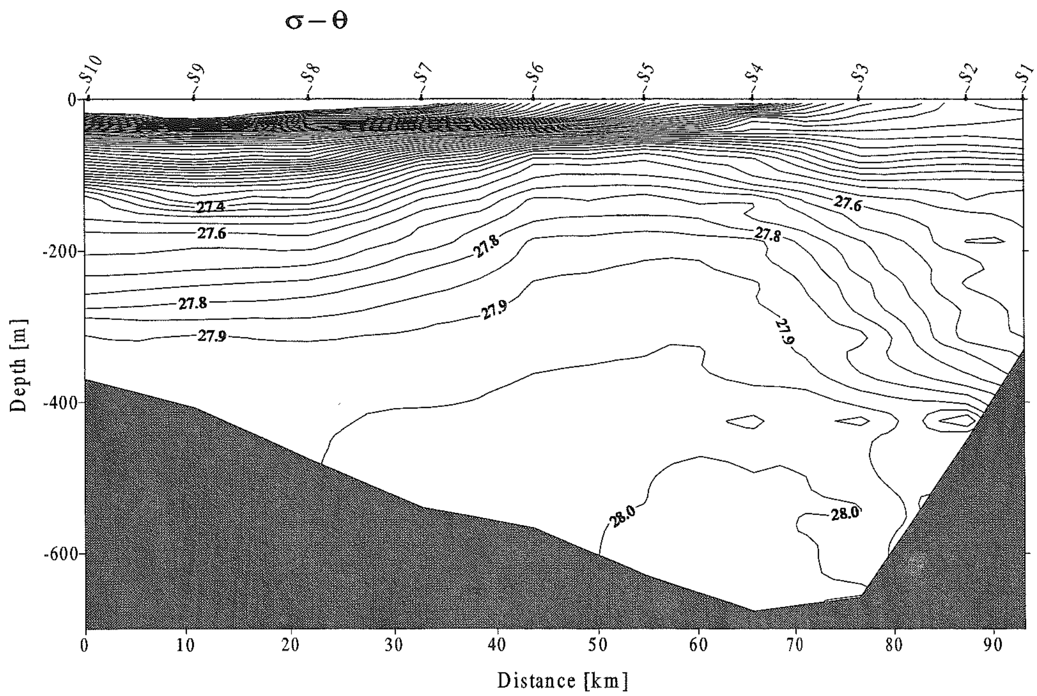

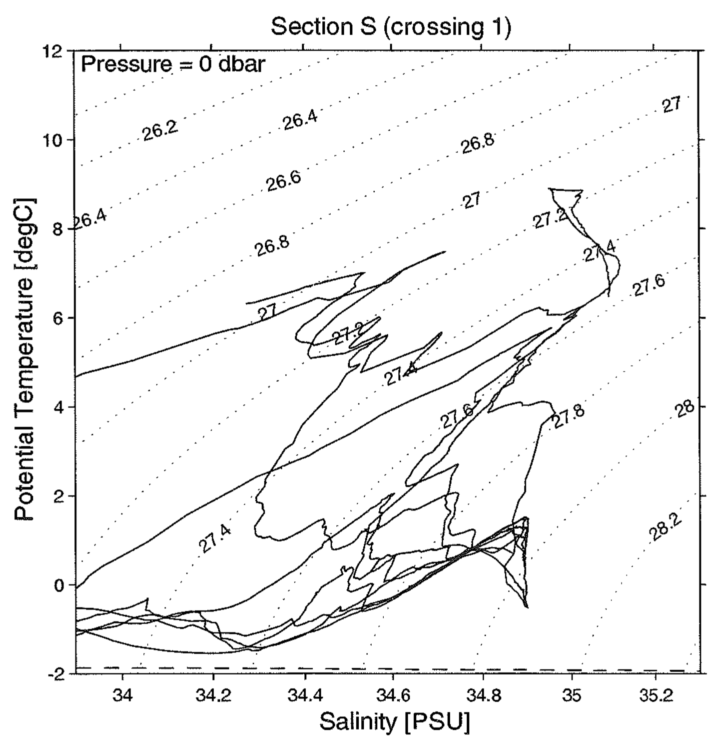

Section S, crossing 2

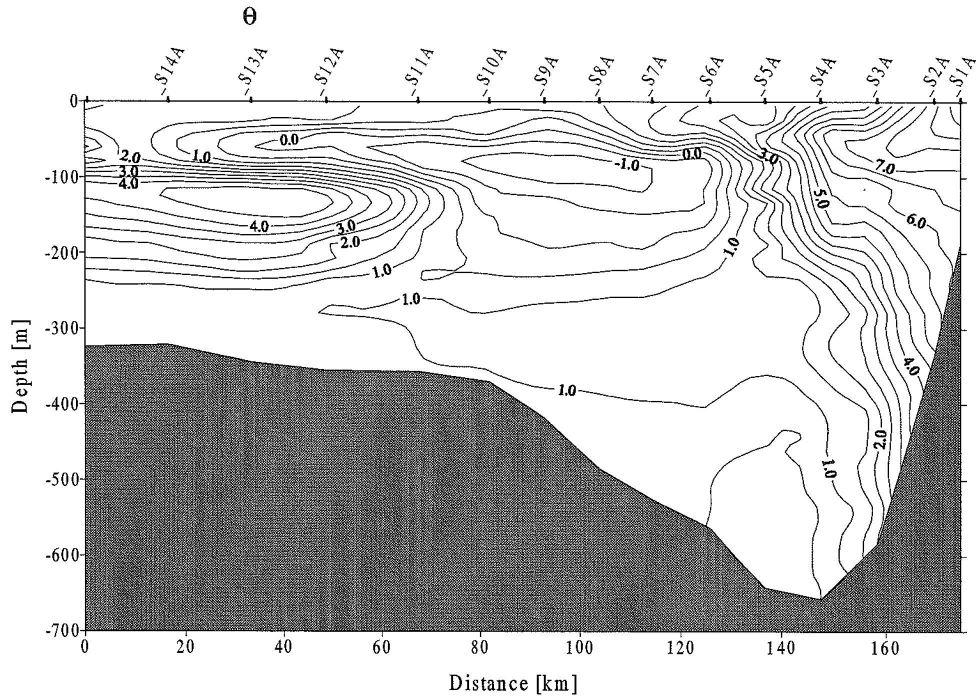

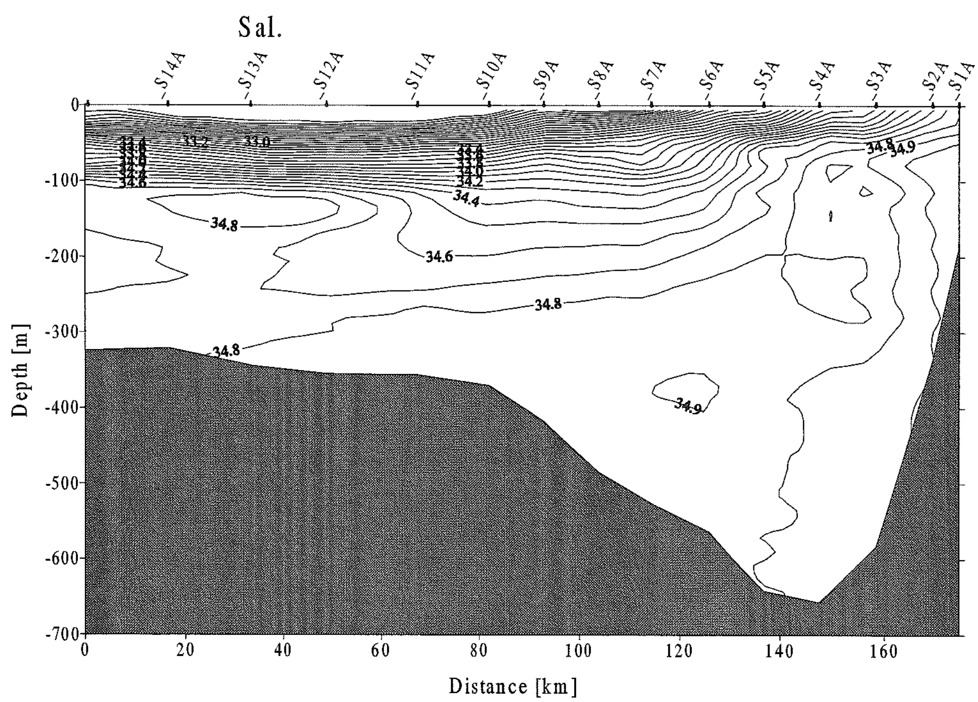

Section S, crossing 2

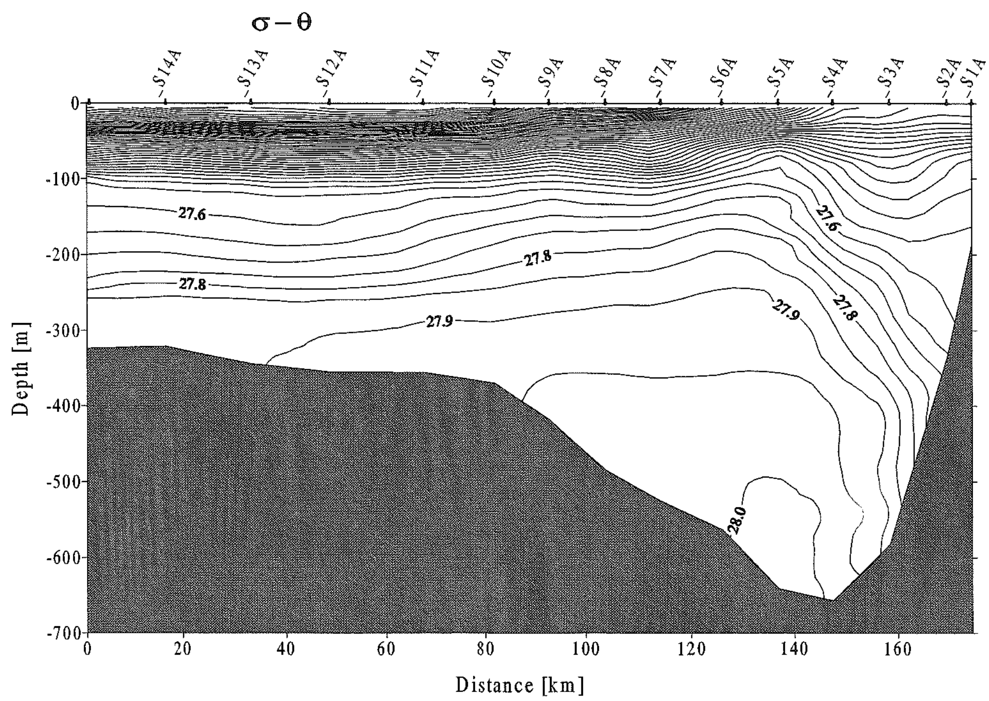

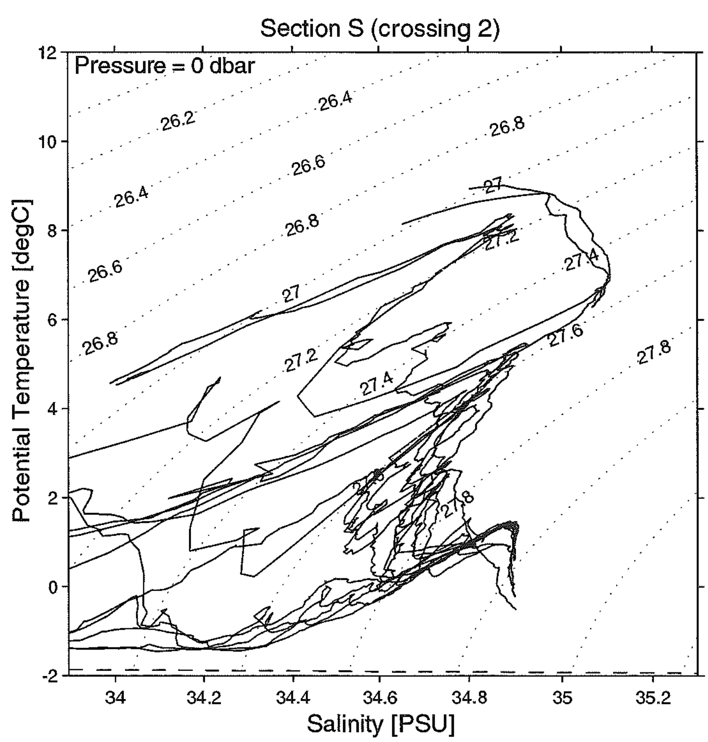

HYDROGRAPHIC OBSERVATIONS IN DENMARK STRAIT ON THE VEINS EXPEDITION WITH RV ARANDA IN AUGUST-SEPTEMBER 1997

TECHNICAL REPORT

APPENDIX B

Listings of temperature, potential temperature, salinity, density (σ_θ-1, σ-2, σ-4σ), dynamic depth, specific volume anomaly and depth for standard pressure levels, and profiles of potential temperature, salinity and σ_θ (0-3000 db, and blow-up of the deepest 500 dp), and Potential Temperature-Salinity diagrams (full scale and blow-up) for each station.

This appendix (301 pages) is available upon request from the Finnish Insitute of Marine Research.

No. 39 Hydrographic observations in Denmark Strait on the VEINS expedition with RV Aranda in August-September 1997 - Technical report

Merentutkimuslaitos
Lyypekinkuja 3 A
PL 33
00931 Helsinki

Havsforskningsinstitutet
PB 33
00931 Helsingfors

Finnish Institute of Marine Research
P.O. Box 33
FIN-00931 Helsinki, Finland

ISSN 1238-5328 ISBN 951-53-2082-8